Generalized Simulation and Processing of TAP Reactor Pulses

A Thesis
Presented to
The Academic Faculty

By

Adam C. Yonge

In Partial Fulfillment
Of the Requirements for the Degree
Master of Science in the
School of Chemical and Biomolecular Engineering

Georgia Institute of Technology
March 2019

May 2, 2019

Generalized Simulation and Processing of TAP Reactor Pulses

Approved by:

Dr. Andrew J. Medford, Advisor
School of Chemical & Bimolecular Engineering
Georgia Institute of Technology

Dr. Tobin Issac
School of Computational Science & Engineering
Georgia Institute of Technology

Dr. Carsten Sievers
School of Chemical & Bimolecular Engineering
Georgia Institute of Technology

Date Approved: March 26, 2019

Acknowledgments

Special thanks is given to Dr. A.J. Medford for his guidance and patience throughout the evolution of the project. Not only did he make great suggestions and offer critical insights, but he was also remarkably kind while doing so. Further, thanks is given to Dr. Tobin Issac, who suggested FEniCS and often took valuable time to answer questions and provide assistance. Thanks is also given to Dr. Carsten Sievers, who provided considerable advice in kinetic modeling and provided insight into the chemistry underlying the mathematical models.

This thesis would not be possible without the past and continuing development in the TAP community. Drs. Rebecca Fushimi and Ross Kunz of Idaho National Labs have been collaborators for the duration of the project and helped introduce us to the field and assisted in the development of this program. Even further, TAP research groups across the country, including Dr. Christian Reece of Harvard University and Drs. Grigoriy Yablonksy and John Gleaves of Washington University in St. Louis, provided us with independently developed TAP simulation scripts. This helped with validation and provided a strong starting point for the thesis.

I would also like to thank Dr. Andreas Heyden and his research group, who provided me with countless opportunities for personal and academic development. Without his outreach and the guidance provided by him and his graduate students, I likely would have never performed research.

Last, thanks is given to my friends and family, who frequently provided much needed moral support.

The research presented in this thesis was funded through a grant from Idaho National Labs. We declare no competing financial interest.

Contents

List of Figures

List of Tables

List of Symbols and Abbreviations

TAP . . . . . Temporal Analysis of Products

RRM . . . . . Rate Reactivity Model

MARI . . . . . Most Abundant Reaction Intermediate

$\boldsymbol{C}_i$ . . . . . Concentration of Gas Species i

ε . . . . . Void Fraction of the Inert or Catalyst Material

$\boldsymbol{D}$ . . . . . Knudsen Diffusion Coefficient

$\boldsymbol{R}$ . . . . . Rate Expression

θ . . . . . Surface Coverage of Species i

δ_t . . . . . Dirac Delta Function i

L . . . . . Length of the Reactor i

Ω . . . . . Subdomain of the Reactor

DFT . . . . . Density Functional Theory

E-R . . . . . Eley-Rideal Reaction Mechanism

L-H . . . . . Langmuir-Hinshelwood Reaction Mechanism

F_i . . . . . Outlet Flux of Species i

k_j . . . . . Rate Constant j

N_T . . . . . Total Number of Iterations

TST . . . . . Transition State Theory

MKM . . . . . Microkinetic Model

DRC . . . . . Degree of Rate Control

***** . . . . . Active Site

Summary

An understanding of intrinsic kinetics is necessary for the rational design of new materials for catalytic processes. One way to obtain this information is by running and interpreting Temporal Analysis of Products (TAP) reactor experiments. Though these experiments provide rich, transient kinetic information, converting the raw TAP data to knowledge of the material is a major bottleneck. Steps have previously been taken to reduce this burden, but further developments, as well as refinement of current methods, are needed. One change that could improve processing is the application of automatic differentiation (AD), which offers a highly accurate calculation of the derivative. For this reason, a workflow to simulate and process TAP reactor pulses built around the FEniCS Python package has been developed. This package allows for the efficient evaluation of the necessary PDEs for TAP, and allows for efficient AD by taking advantage of the adjoint operators of the PDE.

A method to convert elementary reactions directly into the FEniCS PDE format was developed. The first steps to generate reaction mechanisms, as well as sets of rate-limiting reaction expressions, based on the gaseous reactants and products observed during TAP experiments were also taken. The new, general method of simulating pulses around FEniCS was validated and benchmarked. The time required for each simulation was not found to limit the workflows ability to quickly handle TAP data, but improvements can be made.

The Degree of Flux Control was also introduced as an alternate form to the commonly used Degree of Rate Control. This is the first example of a transient sensitivity analysis performed on TAP pulses, and one of few implementations of the Degree of Rate Control analysis to transient processes.

A method to fit parameters was also implemented, and objective functions were constructed with a reduced number of points to improve efficiency.

The parameter fitting method was applied to several examples, including pure diffusion, a linear reaction mechanism, and multiple carbon monoxide oxidation reaction mechanisms, and was found to accurately determine diffusive and kinetic parameters.

The methods developed in this Thesis show the utility of AD and should lead to a more efficient processing of TAP data. This workflow will act as a foundation on which more advanced methods can be developed, including forward and reverse uncertainty quantification, the generation of initial parameter estimates for fitting, and the application to increasingly complex reaction networks. Ultimately, it is envisioned that these methods can work in concert with experiments, providing

a route to adaptive TAP experiments that automatically interrogate the intrinsic kinetics of real catalytic materials.

1 Introduction

Catalyst selection and optimization is a necessary step in the design of many chemical production facilities[1]. Determining an appropriate catalyst for a process, however, is often challenging due to the vast number of variables affecting the catalyst and its environment[2]. Before determining appropriate production-scale operating conditions, the choice of catalyst support[3], composition[4], cluster size[5;6], and solvent[7] must be considered to optimize product selectivity and yield. Even mild changes to catalyst performance can result in multi-million-dollar profit shifts or to necessary reductions in pollutants[8;9;10]. Gaining a robust knowledge of intrinsic kinetic parameters can lead to the rational design of both the catalyst and reactor. For these reasons, methods to efficiently probe the kinetic properties of catalysts have been, and continue to be, developed.

Solving for kinetic parameters through reaction model fitting is a standard approach in the field of catalysis[1]. Typically, data is collected at steady state and fit to equations through simplified Langmuir-Hinshelwood or Eley-Rideal kinetic models. Plotting the extracted kinetic parameters with an Arrhenius equation can provide insight into the apparent activation energy of the process. Though valuable insights can come from this method, the rate limiting step will dominate the extracted kinetic information, resulting in little insight into other elementary reactions in the system. Density functional theory (DFT)[11] calculations, transition state theory (TST)[12] and micro-kinetic modeling (MKM)[13] are frequently used to gain fundamental insights about the thermodynamics and kinetics of reactions on catalysts that traditional experiments are unable to provide. Though these methods can provide users with information pertaining to the mechanism[14], turnover frequency[15], molecular orientation[16] and stability[17], running simulations with DFT requires significant computational resources, even for relatively simple systems[18;19]. To overcome this challenge, DFT calculations have been used to develop theoretical trends, like linear scaling relations[20;21] and volcano plots[22], to help investigators identify more active catalysts in an efficient manner[23;24]. Even with these improvements, it is still challenging to extrapolate information to other surface cleavages, materials, coverages and environments. This is a major obstacle, since materials of interest can have many potential active sites, often with only one dominating the observed reaction rate[25]. If time requirements and system complexity had little impact on theoretical investigations, the inherent error in the electron exchange-correlation approximation is high[26] and makes it challenging for users to draw strong conclusions about results[27]. The associated error in determining transition states alone is between 0.2 and 0.3 eV, meaning that the identification of dominant reaction paths might not be possible with the current state of DFT[28]. New data processing methods merged with experiment could help patch some of these limitations.

Transient experiments can give a broader understanding of the kinetics at play in a system by providing information about each of the elementary reactions and the rate of consumption or production of each species involved[29], but effectively decoupling the transport and kinetics is often cumbersome[30]. The temporal analysis of products (TAP) reactor system was developed to combat this issue. Originally conceived in 1977[31;32], TAP is a surface science technique with approximately twenty systems worldwide (five of which are in the United States). One reason it remains in limited use is due to challenges with data processing. Through the years, steps have been taken to reduce data complexity and make data analysis more efficient.

First, the reactor was modified to include a thin-zone of catalyst packed between two large inert zones[33;34], allowing for a new method called the Y-procedure to be implemented. The Y-procedure[35] was developed to help users determine gas phase concentrations and reaction rates in the thin catalytic zone without making mechanistic assumptions. Since diffusion is only occurring in the inert zone and the boundary conditions are well defined, it is possible to use a fast-Fourier transform to trace the flux and concentration back to the catalytic zone. These implemented boundary conditions and the transformation process are the two components that make up the Y-procedure. The concentration gradient is negligible at low conversion because of the thin-zone experimental setup, so the rate of reaction can be determined by comparing the flux at the entrance and exit of the catalytic zone . This method of determining the rate is similar to that used by the continuously stirred tank reactor (CSTR) model, where perfect mixing is assumed and a uniform concentration exists in the reactor. Post-processing of data with the Y-procedure also allows the surface uptake to be measured as the integral of the rate while accounting for the stoichiometry[36].

Second, the Rate-Reactivity Model (RRM)[30] was developed to provide the user with phenomenological information that could be linked to the kinetics without requiring the user to define some reaction mechanism. The RRM is a linear model and assumes reactions measured by the TAP reactor are first order. The RRM is well suited to take information from the Y-procedure and show how the reaction rate depends on the observed concentrations and surface uptakes in the catalyst region over time. This can provide users with insights about the mechanism, as well as impose constraints used to limit the number of possible mechanisms. Even though these advances have made TAP output data more useful, further steps must be taken to fully utilize the information contained in TAP data.

An over arching workflow has been developed (Figure 1) and shows current data analysis processes used in the TAP community alongside some proposed methods. The core of this workflow is the TAP simulator (component B of Figure 1), which can provide synthetic data for the validation of new methods (component E of Figure 1) and be used for parameter optimization purposes.

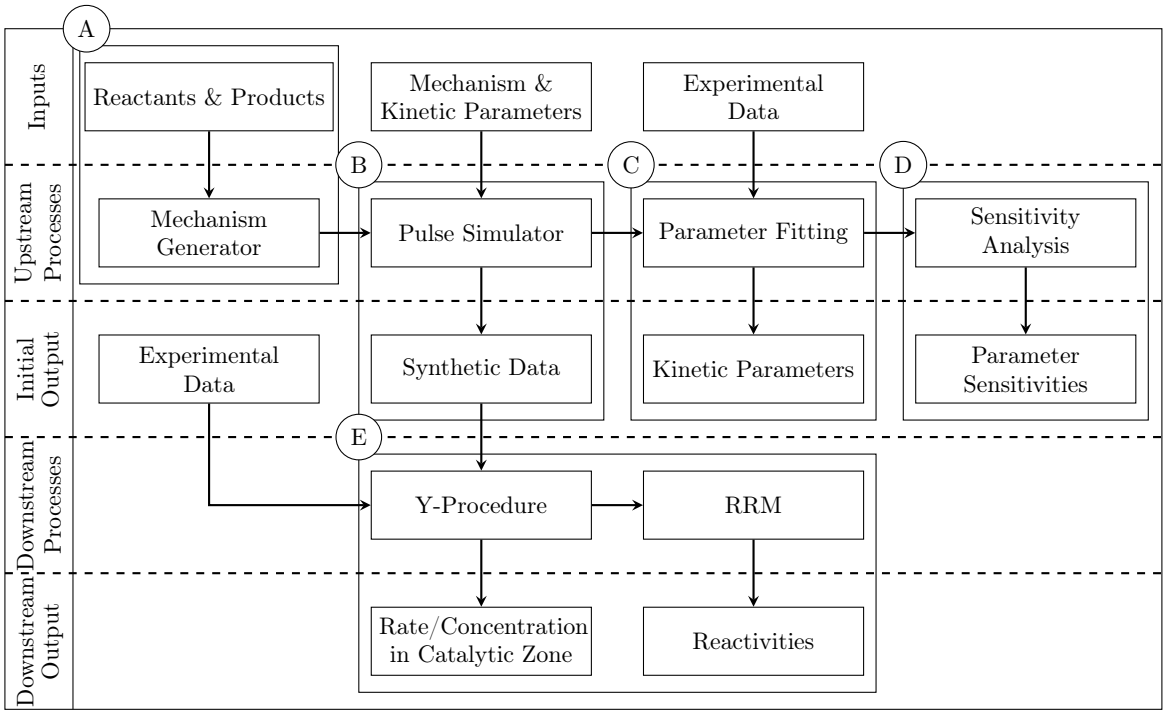

Figure 1: Workflow showing common and new methods to process TAP reactor pulses. Component A shows a method to generate sets of elementary reactions based on the gas species monitored during the pulse. Component B shows the pulse simulator, which can take reaction mechanisms from component A or directly from the user. Component C shows the parameter fitting method, which works with the simulator to determine parameters for the reaction mechanism. Component D is the sensitivity analysis, which can help identify rate limiting steps throughout the duration of the pulse. Component E shows the Y-Procedure and Rate-Reactivity Model, which are common experimental processing methods. Developing more efficient, open source forms of components A - D is the main thrust of this Thesis.

Having to define the reaction and transport equations for any reactor system can be tedious, time consuming and lead to simulation errors or inaccuracies. The simulators used in the field are often geared toward very specific reaction mechanisms. Golman et al. developed a TAP simulator for carbon monoxide reactions, but it was designed for educational purposes and is not meant for processing TAP data[37]. The TAP simulation package TAPFIT can be used for general reactions, but has limited use based on the flexibility of the code and can be cost prohibitive[38]. Further, a generalized mechanism generator (component A of Figure 1) has not been implemented in the field and could help establish multiple reaction networks with limited user input.

As mentioned, the pulse simulator is an intrinsic step in parameter fitting (Component C of Figure 1). The ability to directly fit kinetic parameters to physically meaningful models (i.e. microkinetic models) would be a useful addition to the TAP processing catalog. The primary challenge in implementing a parameter fitting method is handling the intense volume of data from each TAP experiment, which can consist of four-hundred separate pulses with millisecond time resolution. Fitting kinetic parameters to multiple mechanisms for each and every pulse is

infeasible with traditional optimization methods when no strong initial guess is made. One way that efficiency can be improved is through the application of automatic differentiation (AD)[39].

The evaluation of derivatives is necessary for modeling physical systems, as well as for solving optimization problems. Symbolic differentiation is an ideal method for working with derivatives, but is challenging to implement programatically[40]. Taking derivatives by hand may be more efficient for certain problems, but the chance of human error is higher and equations can become difficult or impossible to derive. Numerical differentiation is often used, but will result in a loss of precision and increased computation time[41]. AD offers a middle ground between numeric and symbolic differentiation through the application of the chain rule. By deconstructing equations into less complicated functions, AD allows a computer to evaluate derivatives through simple operations. The two common implementations of automatic differentiation are forward and reverse mode. The former allows the user to evaluate the derivatives of an output function with respect to inputs based on known parameters, while the latter allows the user to determine derivatives of input parameters based on an output. AD has successfully been applied in a variety of fields, including geophysics and finance, and could prove to be useful when applied to catalysis[42;43;44].

The derivatives generated with AD can also be used to perform sensitivity analyses (component D of Figure 1) on known or proposed reaction mechanisms, providing information about rate limiting steps during the progression of a TAP pulse. The standard implementation of sensitivity analysis in the catalysis community is through the Degree of Rate Control (DRC) developed by Dr. Campbell. DRC analyses are typically performed on steady state microkinetic models and only a few have been applied to transient kinetic processes. This is not surprissing, since evaluating derivatives can be costly and at times inaccurate. No transient sensitivity analysis has been performed on TAP pulse models and the use of accurate derivatives could make it possible.

One available tool that allows users to incorporate automatic differentiation into the analysis of partial differential equations (PDEs) is the FEniCS[45] python package. FEniCS acts as an 'umbrella' for other scientific computing packages, some of which include Dolfin-Adjoint[46;47;48;49;50], UFL[51], and PETSc[52]. Beyond the availability of automatic differentiation in the program, FEniCS makes it easier to convert a physical model into finite-element code, while still giving users the flexibility to solve more complicated problems. FEniCS has been used by many groups in a broad range of disciplines[53;54;55;56;57], but, to our knowledge, has seen little to no application in chemical engineering or catalyst design and optimization.

In this thesis, a FEniCS based TAP pulse simulator is developed and acts as the cornerstone on which other methods will depend. A method to generate simple reaction mechanisms and rate

expressions is included to simplify the specification of reaction expressions in FEniCS. Comparisons to simulated data from other groups is made to validate the transport and reaction terms. The efficiency of the simulator and sensitivity analysis will also be discussed. Synthetic data is generated for several carbon monoxide oxidation reaction mechanisms to show the simulators versatility. A sensitivity analysis is also be performed as the first steps taken to develop a method of DRC. A method to fit kinetic parameters to micro-kinetic models will also be introduced and applied to simple examples and carbon monoxide oxidation. The major benefit of this code are be that a plethora of information can be gained with limited user input. Manually defining the PDEs will no longer be necessary when analyzing TAP pulses. Developing an efficient, but thorough, method to simulate and process data will allow the user to rapidly gain valuable insights from complicated systems and could be integrated into a TAP data workflow[58].

2 Handling Elementary Reactions and Reaction Expressions

2.1 Method to Automatically Generate Relevant Partial Differential Equations from Elementary Reactions

The generalization of the TAP pulse simulator is a necessary step toward the development of a more versatile tool that can be integrated with the current data analysis workflow [59]. Simulations will involve unknown mechanisms and an undetermined number of gas and surface species, meaning that defining a library for all potential mechanisms would be impractical and of limited use. For this reason, a method to convert a set of elementary reactions to the necessary PDEs has been developed. These equations can be applied directly to the FEniCS pulse simulator.

2.1.1 Rules for Expressing Elementary Reactions in the Simulator

The elementary reactions being fed to the PDE equation generator must follow a specific structure. The current format of the elementary reaction needed to generate the PDEs is rigid and a few formatting issues, as well as the nomenclature, must be specified. The asterisk (*) indicates an open surface site and (species)* indicates some adsorbed species. The order of the adsorption processes is important; reactant gas species must be specified first. This requirement stems from the way the script will later have pulse intensities specified. Only forward and reversible reactions can be interpreted by the parser. Though the inclusion of an irreversible reaction may seem counter intuitive to understanding the intrinsic kinetics, it is a common method of specifying an elementary reaction and including it as an option further improves the simulators ability to handle a variety of user-defined mechanisms. Some elementary reactions are also much faster in the forward direction, meaning the reverse rate will play a negligible role in the mechanisms and observed rate, leading to a more efficient simulation.

The elementary reactions defined by the user are fed to the script as a list of strings. Each string is then parsed for gas and surface species, as well as the stoichiometry. Each species is added to a list, which is then organized based on whether it is a gas (appearing in the front of the reaction) or surface species (appearing at the end). A matrix specifying the reaction stoichiometry for each elementary reaction is then generated, with rows representing each elementary reaction and columns representing each species. This matrix is used to define the rate of reaction provided in the list of elementary reactions. If the species does not include an asterisk, then the additional diffusion transport term will be included alongside the elementary reaction terms of the PDE. The rate constants for each elementary reaction follow zero-based indexing the traditional numbering

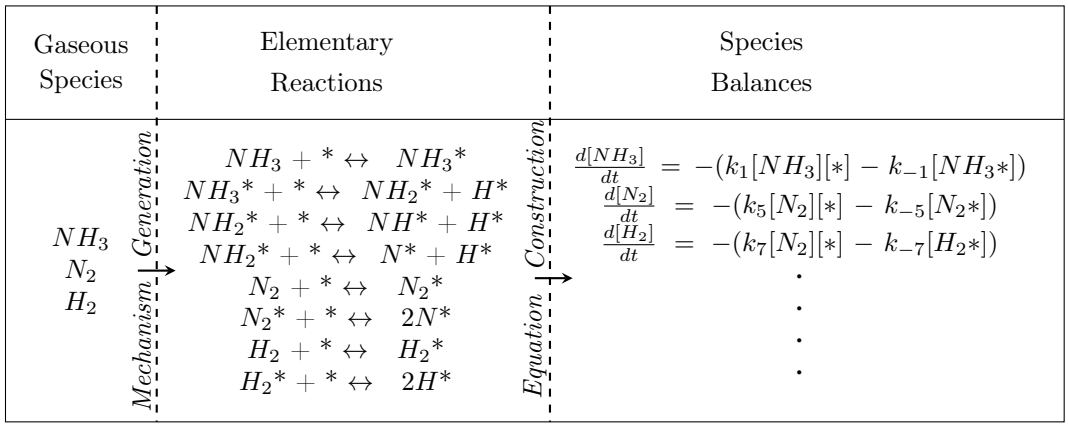

Figure 2: A visual for the inputs and outputs from the mechanism generator and elementary reaction processor. Users will be able to specify the observed gaseous species in future implementations and generate a set of elementary reactions. Once the elementary reactions are specified (either directly from the user or through the mechanism generator), the species balances can be generated and incorporated in the PDEs.

system in computer science.

2.2 Method to Automatically Generate Sets of Elementary Reactions

Automatically generating mechanisms is not a new topic[60;61]. The Rule Input Network Generator (RING) describes all possible reaction paths and performs a subsequent analysis to determine dominant reaction paths and thermochemical properties of the system, while the Reaction Mechanism Generator for Heterogeneous Catalysis (RMG-Cat)[62] determines potential reaction paths through the application of binding energy and Brønstead-Evans-Polanyi relationships. These tools greatly reduce the time required for building and evaluating large reaction networks. However, the associated error and challenge of evaluating excessively large reaction networks, commonly found in heavily oxygenated biomass molecules, limit their broader application. A refined, simpler version of these tools that does not incorporate energy estimates or complex rule inputs will enable useful in generating sets of elementary reactions and subsequently the PDEs necessary to perform TAP pulse simulations.

Medford et al. have developed an in house mechanism generator that uses PyBel[63], a package used to generate molecular objects in python, and Networkx[64], used to handle tasks related to graph theory[65;66]. Unlike other generators, exhaustively probing a reaction network is not the goal. Establishing more compact reaction networks toward desired products is the primary focus, which reduces the chance of the reaction network reaching an uncontrolled expansion. Figure 2 shows the desired conversion between the reactants/products and elementary reaction equations, which requires enumerating the mechanism and converting to equations.

2.2.1 Rules and Challenges with Generating Mechanisms

To use the network and elementary reaction generator, a set of gaseous species must be provided as reactants and products. The network generator also gives the option to specify some reactive intermediate in which the network will flow through. This will be very useful for complicated molecules (like longer chained carbon species) where a direct path might not be clear.

Alongside the standard surface reactions, direct gas interactions with open surface sites and adsorbed species will be considered. It is desired to make a relatively simple mechanism involving the adsorption and decomposition of these molecular species. Though a method to iteratively cleave bonds was developed, it is necessary to convert the set of bond cleavages into a list of elementary reactions that can be interpreted by the user and properly read by the TAP simulator.

Reactions that fall in the Eley-Rideal vein can be difficult to incorporate programmatically. Not every combination of gas and surface species interaction will need to be considered. If they were, there would be an unnecessary increase in the number of reactions that would severely increase simulation time. It's possible to assume that gas species could only interact with the most abundant surface intermediate (MARI), but this would require a prior understanding of the surface composition which is frequently unknown. For this reason, it will be necessary for the user to include these reactions alongside the reactant inputs. Unfortunately, there is no rule the program could currently follow to assume which reaction will interact most with adsorbed species, but the user's intuition and required input is limited.

This script can generate the necessary elementary reactions needed to define a reaction mechanism, though it has not been applied to the simulator and currently acts as a stand alone process. Additional steps must be taken to fully utilize the network generator. First, a method to split the generated elementary reactions into separate mechanisms is needed. In addition to isolating reaction paths, the option to include active sites needs to be provided as an option. Though reaction networks can be generated, it is still necessary to convert them into elementary reactions that can be used by the TAP simulator. This can be achieved by performing the experiments and observing what products are formed, rather than relying on chemical intuition. With the study of more complicated molecules[21;67], an improved mechanism generator will likely be needed.

2.3 Generating Steady-State Reaction Expressions from Elementary Reactions

A method to generate reaction equations based on the concept of rate-limiting steps has also been developed. This script takes in a set of elementary reactions and iteratively assumes that each one of the steps is rate-limiting and all others are in quasi-equilibrium, storing a reaction expression for each one assumed. Sympy[68] was used to manipulate each of these equations and isolate variables while generating the rate expression. At times, the script is unable to isolate the expression due to algebraic issues in Sympy. When this occurs, the user will be notified of the error and the script will continue to generate rate expressions for the remaining rate-limiting steps.

The rate-limiting step generator has also not yet been incorporated into the TAP pulse simulator. Symbolically manipulating these equations with Sympy is inefficient and new methods could be used in future implementations of the program. Though including a rate-limiting step option for users would be an interesting option for improving efficiency, it was not immediately necessary. This feature will be offered in future versions of the package.

3 TAP Pulse Simulator

3.1 The TAP Reactor Setup

Having a firm understanding of the reactor setup and what is being monitored is a crucial step to fully appreciate TAP experiments. Figure 3 provides a simplified visual of a TAP reactor. The thin-zone TAP reactor includes two equally sized inert zones on each side of a thin catalytic zone. An inert zone is placed at the beginning of the reactor to allow the pulse to disperse uniformly in the radial direction. It has been shown that a one-dimensional model is acceptable when the length of the micro-reactor is at least three and a half times the radius of the reactor [69]. A length below this has the chance of having radial and axial dispersion occurring simultaneously. Figure 4 shows how the TAP reactor is discretized for one dimensional simulations. This simplification reduces the complexity of the equations and the computational burden on the associated solver. The catalytic zone is made to be small (typically near one twenty-eighth the size) to reduce the concentration gradient along the region. This "thin-zone" setup is preferred because it facilitates the Y-Procedure analysis through better understanding of the transport.

The molecular pulse introduced to the reactor is commonly of nano-mole size for three reasons. First, the transport of the molecules is well defined, remaining in the Knudsen regime, when the pulse size is kept small. Even when the gas species interacts with the catalytic region, there will be no change in the transport equations or variables. This is a crucial property of the TAP reactor since it helps decouple the transport and kinetics of the system. Second, a limited pulse size helps maintain an isothermal condition inside the reactor. There will be no detectable change in temperature if the reaction is highly endothermic or exothermic when the pulse intensity is on this order of magnitude. Third, introducing a narrow pulse to the TAP reactor will keep the catalyst state, or surface coverage, well defined during each pulse. This is a major advantage and one of the fundamental reasons TAP is desired, allowing users to gradually change the initial catalyst state to a state more likely to be observed industrially. Rather than having an abrupt change in state, a minor shift in the catalytic properties can be detected with each pulse, providing fundamental insight into the role of surface chemistry on reaction kinetics.

3.2 Partial Differential Equations Describing TAP Reactors

The diffusion of a gas species through a TAP reactor, with a general reaction term, can be described as follows:

$$\varepsilon \frac{\partial C_i(x,t)}{\partial t} - \frac{\partial}{\partial x} \cdot (D \, \nabla C_i(x,t)) = R(C_i, k_j, ...) \tag{1}$$

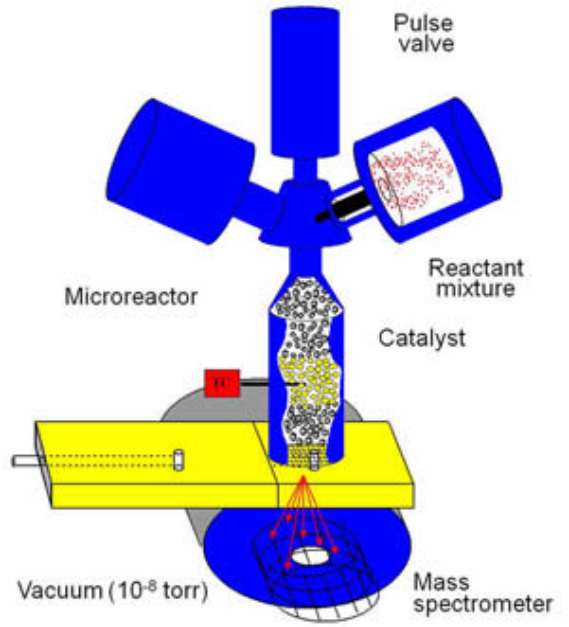

Figure 3: Rudimentary representation of the thin-zone TAP Reactor [70]. A micro-reactor is packed with two inert zones surrounding a thin catalyst region (much smaller than is presented). The reactants are introduce with a pulse valve at the entrance of the reactor and diffuse through the reactor toward outlet, where a vacuum is applied. A mass spectrometer is used to detect the gas at the exit of the reactor.

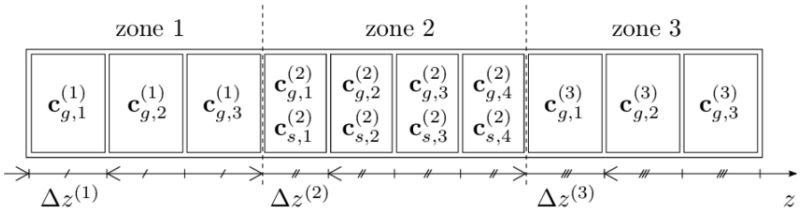

Figure 4: Spatial discretization of a TAP Reactor. The length of the TAP reactor leads to 1-D diffusion through the reactor. Gas concentrations are defined throughout the reactor, but surface concentrations only appear in the second (catalyst) zone.

Where C_i represents the gas species concentration, ε is the void fraction of the inert or catalyst (depending on the section of the reactor), D is the Knudsen diffusion coefficient and R is a combination of the reaction expressions used to describe the transformation of the specific gas species. The reaction term, R, can be expressed as a system of ODEs, or an analytical function, and contains all kinetic information [70].

Many of the molecular species involved in the set of elementary reactions are reaction intermediates that will not leave the surface. Though some form of surface diffusion is likely occurring, it is unlikely to be rate-limiting. For this reason, no diffusive terms are included for surface species and the differential equations can be described as follows:

$$\frac{\partial \theta_i(t)}{\partial t} = R(\theta_i, k_j, ...) \tag{2}$$

Where θ is the surface coverage of species i. The boundary and initial conditions must also be specified to run the simulation. At the entrance of the reactor, a Neumann boundary condition can be imposed due to the use of a pulse valve, which is rapidly opened and closed:

$$\frac{\partial C_g}{\partial x} = \delta_t, \; x = 0 \tag{3}$$

$$C_g = 0, \; x = L \tag{4}$$

Where δ_t is a Dirac delta function and L is the length of the reactor. The flux at the inlet boundary rapidly becomes zero as the simulation progresses. It is important to note that in the finite difference implementations and analytical solution of the program, the exact size of the molecular pulse can be included in the first cell of the mesh. It is also possible to substitute the Dirac delta function approach to defining the pulse with a specific number of molecules in the initial mesh point. Multiple species can be introduced into the reactor system simultaneously, indicated by the index g. When a species is formed in the catalyst region but not pulsed into the reactor, then the flux will be set to zero at the entrance for the duration of the pulse. When more than one pulse is desired, time is reset to zero and another pulse is introduced to the system. Typically, the gas flux for each species is undetectable before an additional pulse is supplied, but there will be a difference in the surface composition from a previous pulse. All gas species will have a concentration of zero at the exit of the reactor due to the applied vacuum conditions, and rate is measured by the flux at the exit.

FEniCS requires users to convert PDEs into the variational, or weak, formulation. A thorough understanding of how to convert equations from strong to weak form is beyond the scope of this work. The variational form used in the simulator is presented below, as verified by FEniCS tutorials[71].

The transport of gaseous species through the TAP reactor in variational form is written as

$$\int \left(\frac{(C_i^{n+1} - C_i^n) v_i}{\triangle t} + D \nabla c_i^{n+1} \cdot \; \nabla v_i \right) dx = 0 \tag{5}$$

where Δt is the size of the time step, v_i is the test function for each of the gas species, and n and $n+1$ are the current and next iteration of the solver, respectively. Reactive terms can easily be added to the RHS of equation 5.

Two subdomains are established in this program

$$\Omega_0 = [0, 1] \tag{6}$$

$$\Omega_1 = [P_1, P_2] \tag{7}$$

The second domain (Ω_1), which represents the catalytic zone, divides the first domain (Ω_0), which represents the inert zones, into two separate regions. Parameters P_1 and P_2 represent the normalized size of the catalyst zone, where the values can be changed based on the size of the catalyst zone. The void fraction and diffusion coefficients, which will vary based on the material, can be specified for each of the zones and applied to each subdomain.

3.3 User Input File

Some users could have little to no experience with Python. To help alleviate this problem, as well as to assist in keeping track of the parameters used for a particular simulation, a csv (or xlsx) file can be used as the simulator input. It will still be possible for more advanced users to work directly with the Python interface and to develop their own processes in the package, but the csv file will act as the primary user input. An example of the input file's structure is broken up into its components in Figure 1. The script reads the input file based on each of the four subsections highlighted in the Figure. Though the order of each row in each of the four sections does not matter, the order in which each section appears does. If a section is excluded or placed in the wrong order, the script will terminate and return an error to the user. If no elementary reactions are provided, the script will also stop executing and return an error upon which the user will be asked to enter the required information.

The first section of the input script is committed to the 'Reactor Setup'. This section controls the basic reactor conditions like length, fraction of the reactor length occupied by the catalyst, temperature, number of time steps and reference diffusion information. The name of the output folder is also specified in this section. It is important for the user to alter the output file name, since keeping the name the same will cause the simulator to return an error and stop running. In future versions of the package, automatically generating these file and directory names may be implemented to avoid this issue. Names describing the temperature, reaction mechanism and overall reaction are likely best for establishing a naming system. The csv file used for the simulation will be copied into the generated folder to keep information organized.

The second section of the input script is the 'Pulse Composition' section. This is primarily

	Input Name	Value	units
Reactor Setup	reactor type	tap	'tap' or 't pfr'
	time	1	seconds
	time steps	1000	———
	mesh size	280	———
	length reactor	3.6	cm
	factor	0.033	———
	temperature	400	K
	void inert	1	———
	void cat	1	———
	reactor radius	0.057	cm
	solver method	1	'0', '0.5' or '1'
	time step option	'None'	'None' or 'S. Adapt'
	ref rate inert	40	———
	ref rate cat	40	———
	ref mass	423	AMU
	output file name	'example'	———
	experimental data	'exp example'	———
Pulse Comp.	reactants number	1	–
	inert pulse size	1e16	molecules
	reactant ratio	1	———
	number of pulses	1	———
	mass list	32,44,40	
	initial surface coverage	0	atoms / cm^2
Output Options	sensitivity analysis	False	———
	display figure	TRUE	———
	save figure	TRUE	———
	store data	TRUE	———
	MKM Analysis	TRUE	———
	RRM Analysis	TRUE	———
	fit parameters	TRUE	———
Elem. Reactions	A -> A*	771.6	1
	A* -> B	2	———

Table 1: The four separate components (reactor setup, pulse composition, output options and elementary reactions) of the input csv/xls file used to simulate TAP reactor pulses. The input variable names, example input values and the typical units (or lack there of) are shown. Offering users the option to fill in the component in a file, rather than alter variables in a script, should make it easier to setup and manage simulations in a directory. For more experienced users, the original scripts are still available for direct editing.

used to control parameters like the size of the inert pulse, the number of reactants being fed, and the pulse intensity of each of these reaction species relative to the inert pulse. This section is also used to specify the initial surface composition, as well as the number of pulses and the mass of the gaseous reactants and products. The surface composition is presented in order of appearance in the set of elementary reactions, with the exception of vacant sites, which will always conclude the list. If multiple pulses are run, the surface composition at the end of a pulse simulation will be the initial surface composition for the subsequent pulse. Similar to the surface composition, the user must specify the pulse intensity of each gas, as well as the number of reactants. If the intensity of each species changes from pulse to pulse, a set of intensities can be provided to the script, each of which is separated by square brackets and commas. This section, as well as the two other sections, are more likely to change between simulations, while the previous section is likely to stay the same between simulations.

The third section of the input script is the 'Data Analysis Options' section, where the user can specify what processes they would like to complete during the simulation. Process options include sensitivity analysis, MKM and RRM analysis. If any of these are defined as true, directories will be generated inside of the folder generated when the simulation began. The names of these directories include 'flux data' for the simulated outlet flux data, 'thin data' for the surface and gas concentrations in the catalyst zone, 'plots' for all the generated figures, 'RRM results' for the results of the Y-procedure and the reactivities found with the RRM, and 'sensitivity' for the sensitivity analysis for each of the gas species for each pulse. The file structure implemented should make it easier for users to locate relevant information without sifting through many, similarly named files.

The fourth section of the input script is the 'Elementary Reactions' section. The elementary reactions defined must follow the same rules specified in section 2.1. The forward rate constant is placed in the first column to the right of each elementary reaction. If the reaction is reversible, then an additional rate constant is included to the right of the forward rate constant. If an elementary reaction is specified and no rate constant is defined, or only a reverse rate constant is specified, the script will return an error and specify that a parameter was not appropriately defined.

3.4 Simulator Validation and Benchmarking

3.4.1 Confirming the Accuracy of the TAP Simulator

Since it is intended for public use, validation of the simulator is a crucial step in development. Without ensuring the synthetic data is accurate, other research groups might avoid using it or, even worse, use it and later find the generated data to be inaccurate. Analytical solutions to the thin-zone TAP reactor have been used to solve for the outlet flux over time for a variety of reaction conditions. An extensive derivation can be found in a publication by Gleaves et al.[69], but the principle behind the method is that a fast Fourier transform can be performed on the differential equations describing each zone. The Fourier transform provides the user with a matrix that takes in a concentration and flux at one end of a zone and returns the concentration and flux at the opposite end of the same zone. This results in a "transfer matrix" formulation relating inlet and outlet concentrations in each zone. A global matrix can then be constructed by combining each of the separate matrices (zones). Upon construction, the user will have the ability to transform the concentration and flux matrix at a particular boundary in one zone of the reactor and trace the solution to another boundary in the system (inlet to outlet, outlet to catalytic zone, etc.). Since outlet flux is what is commonly measured, only a subsection of the expression is necessary with consideration to the boundary conditions: a defined inlet flux and a concentration of zero at the outlet. The problem with these analytical solutions, and the reason simulators are needed, is that they can only be applied to linear systems of equations. This is a major drawback since real catalytic reactions frequently involve non-linear reaction equations. Even with this limitation, using analytical solutions to confirm that transport and simple kinetic expressions are handled correctly will help increase confidence in the simulator.

The data used for validation was provided by Evgeniy et al. The linear reaction considered for validation is species A adsorbing on the catalyst irreversibly (A -> A*) and desorbing as species B irreversibly (A* -> B). An inert is also passed through the system, which acts as an internal reference for diffusion. The diffusion coefficient for each species is set to 20 cm^2/s. The void fraction of the inert and catalyst regions are both equal to 1. Though a void fraction of 1 indicates an empty reactor, having this value will simplify the math, but not diminish the results of the validation. The total length of the reactor is 3.6 cm. The simulation time for the validation data is 4.1 seconds, but the time axis is set between 0 and 1 seconds to give a clearer indication of potential differences between the two. There are no pre-adsorbed species present on the surface either. The rate constants used for each elementary reaction, k_1 and k_2, were set to 1 and 2.

Figure 5 shows the convergence of the FEniCS solution to the analytical solution from the

Fourier transform as the number of time steps increases. Six separate time step sizes were used, including 10, 50, 100, 500, 1000 and 5000. As expected, 10 time steps gives an inaccurate, coarse solution. Simulations with time steps of 50 and 100 have a higher accuracy, but noticeably deviate from the analytical solution. Once 500 time steps are made, the solution curves appear to converge. There is only a minor change in each curve observed between 500 and 5000 time steps. The curves representing the inert and species B do not reach a dimensionless flux value of zero before the 1 second cutoff is made. To show that these curves also converge over the entire 4.1 second simulation, figure 6 is presented. The number of time steps used for these simulations is 2050 and 4100, which coincides with the 500 and 1000 time steps used in figure 5. In general, the FEniCS based simulation curves are indistinguishable from the analytical solution.

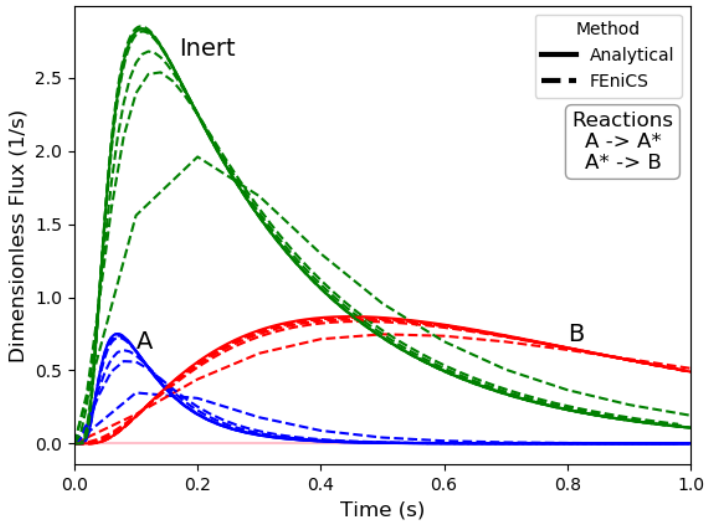

Figure 5: A simulated TAP pulse involving a linear reaction for 10, 50, 100, 500, 1000 and 5000 time steps. The FEniCS curves for A, B, and the inert converged to the analytical solution as the number of time steps increased from 10 to 5000.

3.4.2 Simulation Efficiency

Since a primary aim in developing this package is the efficient simulation and processing of TAP pulses, it is important to gauge simulation time and accuracy at different conditions/mechanisms. This should highlight where improvements are needed in future versions and could help determine optimal simulation parameters for future users. The mechanisms used in this section are defined in table 2, and include the irreversible and reversible adsorption of a single gas species, the irreversible and reversible adsorption of two gas species, the reversible adsorption of two gas species and a three and four step reaction mechanism consisting of three and four gas species. The influence of the number of elementary reactions and reversibility will also be gauged from these examples. Similar

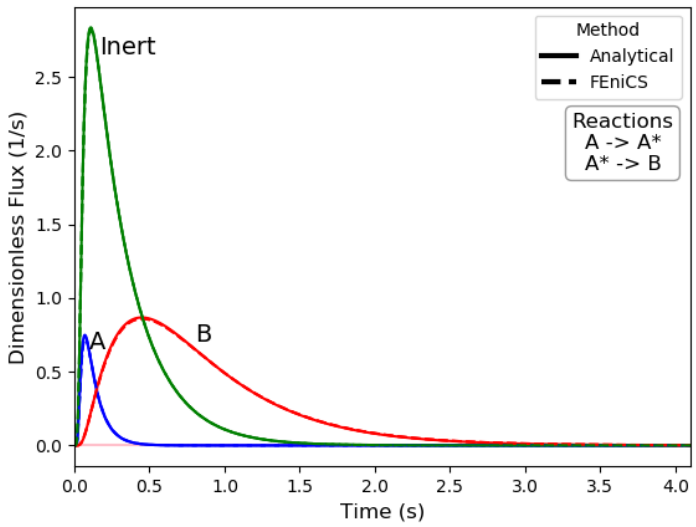

Figure 6: Similar results from figure 5 presented on a time scale of 0 to 4.1 seconds. Two time step sizes, 2050 and 4100, are used to coincide with the 500 and 1000 time steps found in figure 5. No significant deviation from the analytical solution is observed at either scale.

Mechanism	Set of Elementary Reactions	Elementary Reactions
I	1(I)	1 A + * $\leftrightarrow$ A*
II	1(R)	2 B + * $\leftrightarrow$ B*
III	1(I), 2(I)	3 C + * $\leftrightarrow$ C*
IV	1(R), 2(R)	4 A* + B* $\leftrightarrow$ C*
V	1(R), 2(R), 3(R), 4(R)	5 D + * $\leftrightarrow$ D*
VI	1(R), 2(R), 3(R), 4(R), 5(I), 6(I)	6 A* + C* $\leftrightarrow$ D*

Table 2: A set of mechanisms used to investigate simulation efficiency alongside the set of elementary reactions used in each mechanism. 'I' and 'R' next to each elementary reaction represents irreversible and reversible reactions, respectively.

to efficiency analysis for these simple reaction mechanisms, the efficiency will be observed for carbon monoxide oxidation reactions presented in section 4.

The influence of the mesh size on the time per simulation is shown in figure 7. The first four mechanisms show simple linear relations, each getting mildly steeper with the addition of complexity. Adding reversibility to the adsorption of species A causes a minor but noticeable shift in the time requirement. The simulation of two simultaneous, irreversible adsorption process does increase the required time of simulation, but once again it is only a mild shift. When these two adsorption processes are altered to involve reversibility, a minor, almost unnoticeable change in the simulation time is observed. If a third and fourth reversible adsorption process are included, a similar increase in the initial simulation time and change with respect to mesh size would likely be observed. The two relatively complex mechanisms (V,VI) involving surface reactions show a sharp increase in the required time per simulation. The pre-factor increases from the two to three second time range to 11 and 12 seconds. Furthermore, the slope of each is significantly steeper.

Increasing the mesh size for these later mechanisms will result in a longer simulation time than an increase in mesh size for the simpler mechanisms. These two mechanisms are also notably noisy compared to the other two. Where the first four mechanisms show a small increase in the simulation time when going from a mesh size 100 to 500, the last two mechanisms nearly triple from ten to thirty seconds. It seems that the addition of surface-surface reaction causes a significant rise in the simulation time, but adding a second surface-surface reaction does not cause another major shift in the time requirement. To further probe the influence of the mesh size on the simulation time, the required simulation time was monitored for different carbon monoxide oxidation reaction mechanisms in Figure 8. Similar to the general mechanisms, the first, less complicated mechanisms show only mild increases in the simulation time with an increase in the mesh size. The Eley-Rideal mechanism requires the least amount of time over the mesh range, while the Langmuir-Hinshelwood and Langmuir-Hinshelwood/Eley-Rideal mechanisms take similar amounts of time. The more complicated mechanism, which involves four separate reactions, involves more noise and a steeper increase in simulation time with the mesh size.

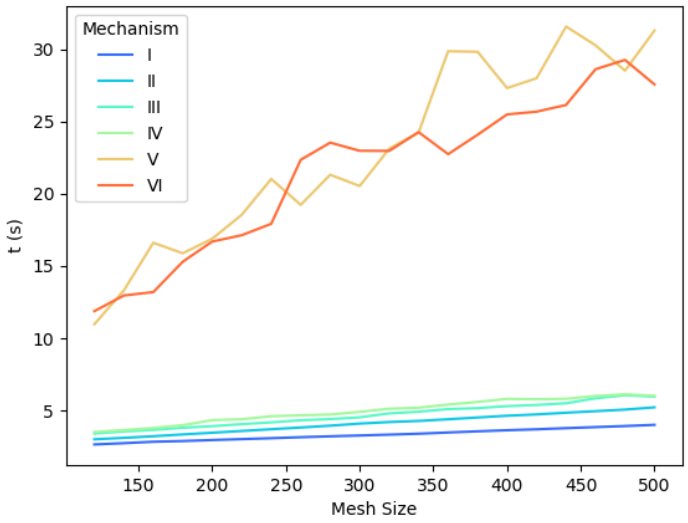

Figure 7: Influence of the mesh size on efficiency for a set of simple reaction mechanisms described in Table 2.

The influence of the number of time steps on the total simulation time for a set of reaction mechanisms are presented in Figure 9. For a small number of time steps, all the reaction mechanisms have similar simulation times. However, as the complexity of the mechanisms increase, the rate at which simulation time increases as the number of time steps increases. The Eley-Rideal (E-R) reaction mechanism requires the least amount of time over the range of time steps, with approximately five seconds being required for a simulation with 1000 time steps. The Langmuir-Hinshelwood (L-H), as well as the Eley-Rideal/Langmuir-Hinshelwood (E-R/L-H), reaction mechanisms show

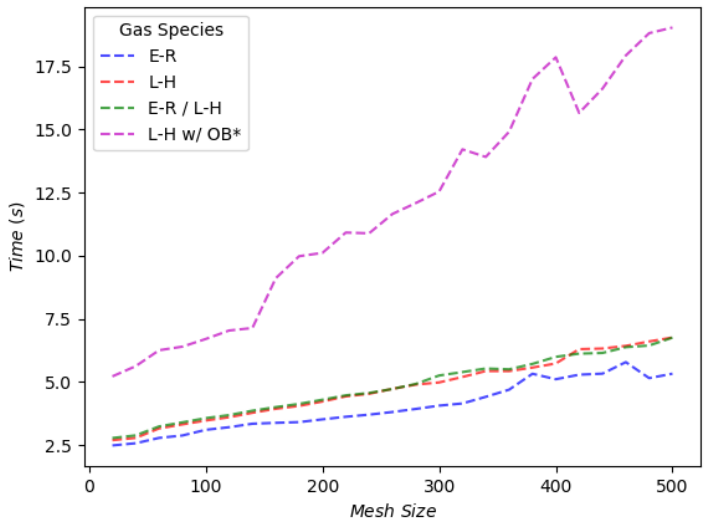

Figure 8: The change in script runtime depending on the mesh size (2 - 1000) for a mesh time step size of 500.

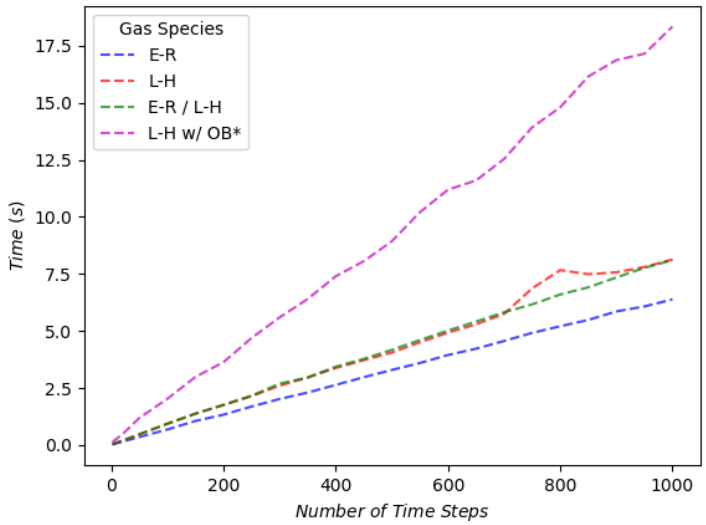

Figure 9: The change in script runtime depending on number of time steps (2 - 1000) for a mesh size of 280.

a noticeable increase in the time requirements with an increasing number of time steps. Finally, the Langmuir-Hinshelwood reaction with the availability of multiple active sites requires the most time by a significant margin. For a simulation involving 1000 time steps, approximately eighteen seconds is required.

It is important to note that the forward mode solver relies on a fixed time stepping method, while other solving methods in the field are able to incorporate adaptive time stepping methods. It is likely that incorporating a method to change the time step would result in significant speed

ups in simulating TAP pulses with FEniCS. Some methods are currently being developed and do show promise[48], but current versions have not yet been implemented in FEniCS. For this reason, the current code has been set up to make it easy to swap out the current time stepping method with an alternative, currently unknown time stepping method. The general goal of the package is to develop a versatile and efficient simulation package for TAP pulses.

Having tested the efficiency of the simulator in terms of the number of time steps and mesh size, two major conclusions can be drawn. First, the time does increase sharply for some mechanisms and more complex mechanisms will likely require finer mesh sizes to properly handle stiffness. Though the choice of mesh and time step size will also depend on the convergence of the curves, a mesh size between 300 and 400 should be acceptable, while a time step size between 600 and 1000 should also be acceptable. Second, the simulation time for fine mesh and step sizes is reasonable. Thirty seconds is an acceptable simulation time, though improvements would be beneficial. One simple fix would be to include a adaptive time stepping method, but, unfortunately, no form of this is available in FEniCS.

4 Application to Carbon Monoxide Oxidation

Due to it's relatively simple reaction mechanism, the catalysis community has often used carbon monoxide oxidation to assist in method development. For this reason, several mechanisms and their kinetic parameters are available in the literature[72]. The types of mechanisms studied include Eley-Rideal (E.R.), Langmuir-Hinshelwood (L.H.) and E.R./L.H. combinations. Each of these mechanisms involve pre-adsorbed oxygen, meaning no oxygen is pulsed in with the carbon monoxide and inert. This could be seen as an unnecessary simplification, but it actually offers two useful illustrations. First, it shows the packages ability to predefine the concentration of surfaces species beyond the standard active sites is available. Second, it gives a glimpse into how the state of the catalyst can evolve with time, since oxygen will be consumed during each pulse. The occupation and consumption of surface species and sites is a common occurrence in TAP experiments and is one of the main reasons smaller pulses can be useful in defining the evolution of the surface.

Synthetic data for each carbon monoxide reaction mechanism was generated with the developed python package. Previously, the user would have to derive and manually enter the equations describing the kinetics and transport of the system. This is no longer true and the user will only have to enter the necessary kinetic parameters alongside the desired elementary reactions.

4.1 Modeling Conditions

The length of the reactor was set to 2.8 cm, with a catalytic zone length of 0.1 cm located at the exact center of the reactor. The radius of the reactor was set to 0.24 cm, which falls within the criteria for 1D modeling[69] and the temperature was set to 400 K. Explicit rate constants were established for each of the following reaction mechanisms, and the diffusivity for each gaseous species are calculated with Graham's law and therefore depended on temperature in the simulator. The masses for each species are provided as a list in atomic mass units. The inlet pulse size was set to $3 * 10^{16}$ molecules and the ratio of carbon monoxide to inert being pulsed in was set to one. All simulations only involved a single pulse, with the exception of the mechanism developed by Reece et. al. Ten separate pulses are included for this model to show that the evolution of the surface can be visualized and to show a more complex case for the sensitivity analysis. The void fraction was set to 0.53 for both the inert and catalyst zones. Each of the simulations involved 600 time steps over a two second window. The mesh size was also set to 280, which was used in the original application of these mechanisms in the TAP community.

4.2 Simulation of CO Oxidation

The first mechanism simulated is Eley-Rideal carbon monoxide oxidation. Consisting of only a single elementary reaction, it involves the direct reaction of gaseous carbon monoxide with pre-adsorbed oxygen species (equation 17). Carbon monoxide does not adsorb on the surface in this reaction mechanism. The dimensionless flux for each of the gas species (carbon monoxide, carbon dioxide and an Inert) are shown in Figure 10.

$$CO + O* \rightarrow CO_2 + * \tag{8}$$

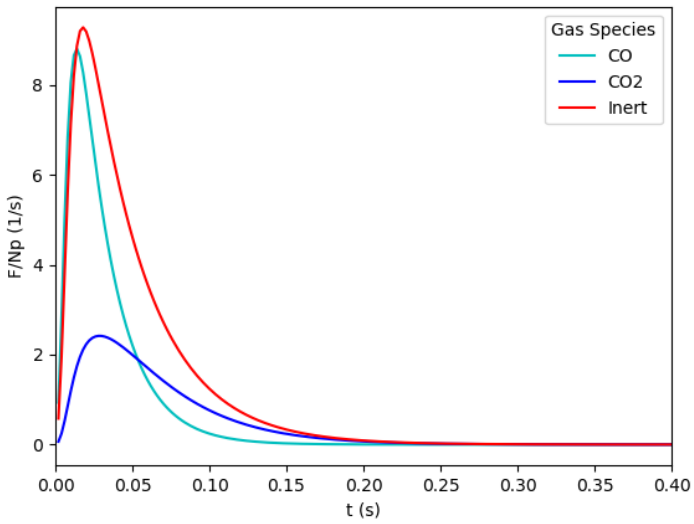

Figure 10: TAP Simulation of CO Oxidation through a Eley-Rideal Reaction Mechanism.

The second mechanism simulated is the Langmuir-Hinshelwood carbon monoxide oxidation. This mechanism consists of two elementary reactions, including the reversible adsorption of carbon monoxide (equation 9) and the subsequent reaction of adsorbed carbon monoxide with pre-adsorbed oxygen species (equation 10). The dimensionless flux for each of the gas species (carbon monoxide, carbon dioxide and an Inert) are shown in figure 11.

$$CO + * \leftrightarrow CO^* \tag{9}$$

$$CO^* + O* \rightarrow CO_2^* + * \tag{10}$$

It is interesting to note the difference in location of the carbon dioxide peaks between figures 10

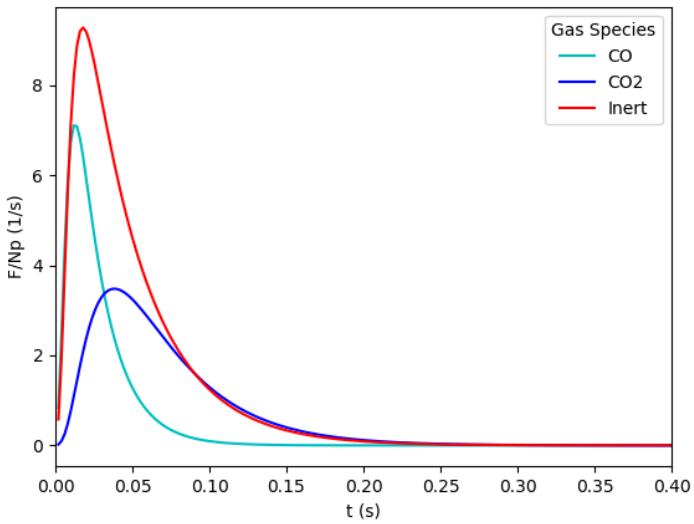

Figure 11: TAP Simulation of *CO* Oxidation through a Langmuir-Hinshelwood Reaction Mechanism.

and 11. In the Eley-Rideal reaction mechanism, the peak is closer to 0.03 seconds, whereas the peak in the Langmuir-Hinshelwood reaction mechanism is closer to 0.05 seconds. This is a previously identified feature in the carbon monoxide reactions, since the formation of carbon dioxide occurs simultaneously with the consumption of carbon monoxide in the Eley-Rideal mechanism, whereas the carbon monoxide is not instantly converted in the Langmuir-Hinshelwood mechanism (i.e. carbon monoxide can linger on the surface before conversion). More carbon monoxide is also consumed in the Langmuir-Hinshelwood reaction mechanism, with lower carbon monoxide and higher carbon dioxide peaks. These qualitative signatures have been used previously for mechanism identification[72].

The third mechanism simulated is a combination of Eley-Rideal and Langmuir-Hinshelwood carbon monoxide oxidation. This mechanism consists of the three previously mentioned elementary reactions (equation 17 to 10) and the subsequent reaction of adsorbed carbon monoxide with pre-adsorbed oxygen species. The dimensionless flux for each of the gas species (carbon monoxide, carbon dioxide and an Inert) are shown in figure 11. With the combination of both reaction mechanisms, both are found to contribute to the conversion of carbon monoxide. The carbon dioxide peak in this figure is noticeably higher than in the previous two, since there are two routes to formation.

The final carbon monoxide oxidation reaction probed involved a Langmuir-Hinshelwood mechanism involving two separate types of pre-adsorbed oxygen types, denoted OA* and OB*. This particular mechanism has been proposed by Drs. Reece and Friend at Harvard based on surface

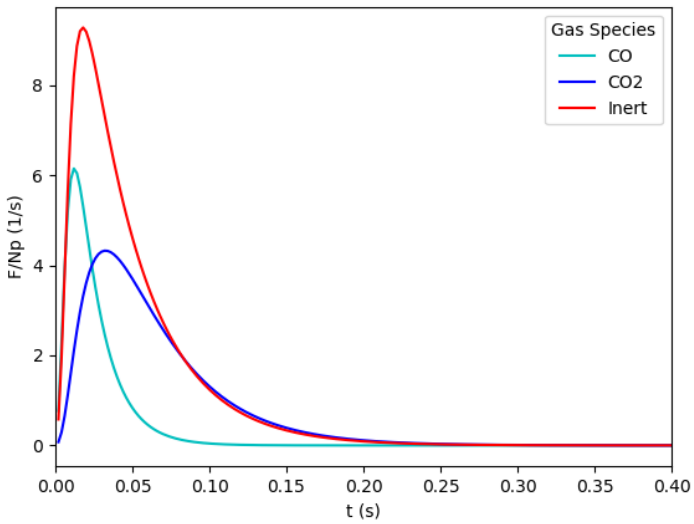

Figure 12: TAP Simulation of CO Oxidation through a Simultaneous Eley-Rideal and Langmuir-Hinshelwood Reaction Mechanism.

science experiments and encompasses elementary reactions 19 to 14. These elementary reactions involve the reversible adsorption of carbon monoxide, the irreversible desorption of carbon monoxide, and the irreversible reaction between adsorbed carbon dioxide and the two pre-adsorbed reactants. There is one major difference between the previous carbon monoxide simulations: no open adsorption sites are defined or included in the elementary reactions. This simplifies the equations, but offers an additional equation type to be considered.

$$CO \leftrightarrow CO^* \tag{11}$$

$$CO^* + OA^* \rightarrow CO_2^* \tag{12}$$

$$CO^* + OB^* \rightarrow CO_2^* \tag{13}$$

$$CO_2^* \rightarrow CO_2 \tag{14}$$

Though these mechanisms are relatively simple, they do show the ability of the workflow to simulate a variety of mechanisms involving different sets of elementary reactions. There are some improvements that can be made (including multiple sites), but the current implementation is flexible enough to handle many common reaction mechanisms.

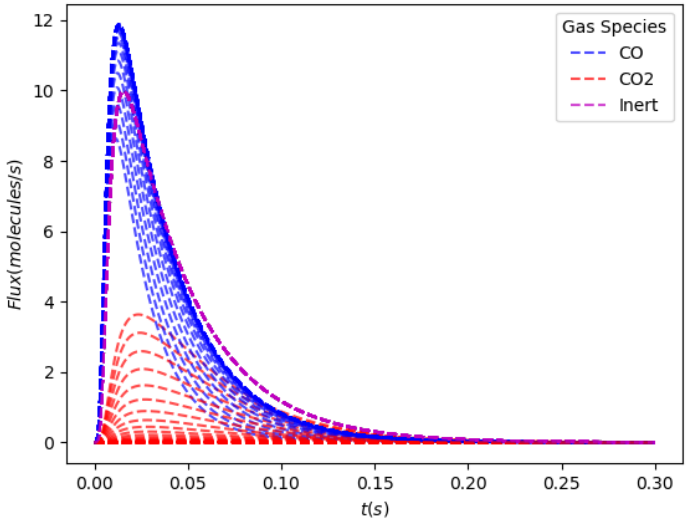

Figure 13: TAP Simulation of CO Oxidation through a Langmuir-Hinshelwood Reaction Mechanism with Two Separate Types of Pre-adsorbed Oxygen.

5 Incorporation of Sensitivity Analyses

A sensitivity analysis is a way for a user to determine the influence of parameters on some desired functions. In the case of TAP reactors, the parameters are the kinetic rate constants and the desired functions are the outlet flux for the monitored gas species. Though a sensitivity analysis is identical to evaluating the Jacobian, there is a use in analyzing sensitivity analyses outside of optimization. Typically, a sensitivity analysis is applied when a user has some confidence in the current values of the parameters. For example, the Degree of Rate Control, developed by Campbell et al.[73;74;75], is the standard in the field of computational catalysis for determining how influential each kinetic parameter is in a set in a set of elementary reactions and acts as a chemically meaningful application of sensitivity analyses. Typically, the DRC method is applied to steady state experiments and relies on the user to manually change parameters and rerun the script. As highlighted by Dr. Campbell himself, this method has had few applications to transient kinetics[74].

A general expression for sensitivity is as follows:

$$DRC = \frac{k_j}{R_i}\frac{\partial R_i}{\partial k_j} \tag{15}$$

where k_j is a particular rate constant and R_i is the rate of reaction or turnover frequency (TOF) of a particular reaction. This form of the sensitivity analysis allows the values to be normalized between -1 and 1, making it easier to draw conclusions about the reaction network. Though possible to apply this directly to TAP with the application of the Y-Procedure, a modified version

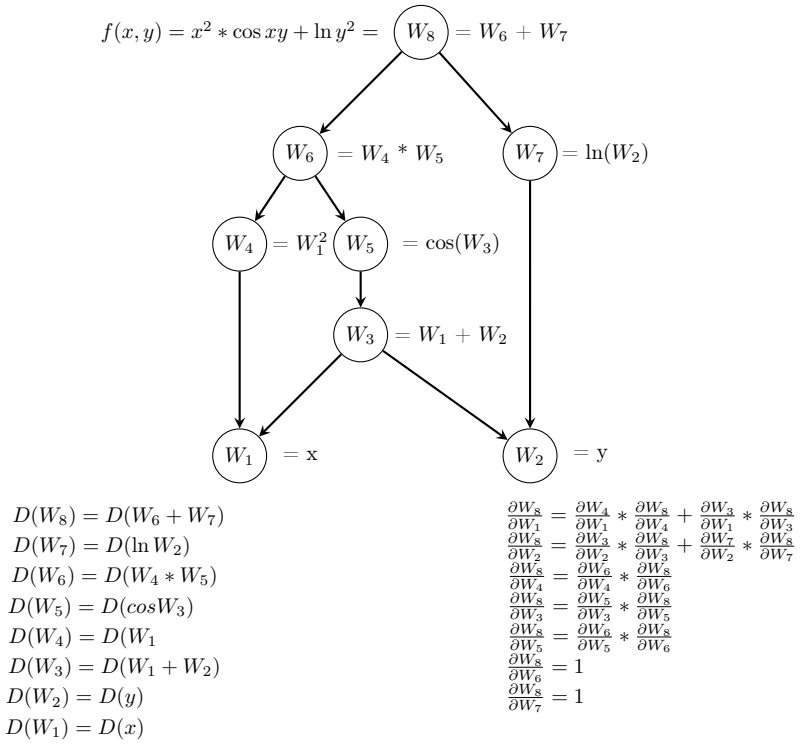

Figure 14: A common visual used to explain the fundamental concept behind automatic differentiation. The above graph shows how a given equation (f) can be decomposed into separate components using the chain rule. The equations in the bottom left show how the derivative expression is constructed. The process will scale with the number of input parameters for constructing the gradient. The equations in the bottom right show how reverse mode AD works, which is a more practical than forward mode when fewer outputs are present than inputs.

of the equation could be more appropriate, written as

$$DRC_{TAP} = \frac{k_j}{F_i}\frac{\partial F_i}{\partial k_j} \tag{16}$$

where F_i is the outlet flux of the reactor. This new form of the Degree of Rate Control is called the Degree of Flux Control, due to its relationship to the outlet flux of the reactor. This type of sensitivity analysis will allow users to observe when rate constants are influential throughout the progression of a TAP pulse over a series of reaction pulses.

5.1 Applying Automatic Differentiation

Automatic differentiation is a unique way to evaluate derivatives, but the underlying mechanics and utility are unfamiliar to most engineers. Figure 14 provides an example of how automatic differentiation works. Some function $f(x, y)$ is specified and its symbolic derivative may not immediately be apparent. It's possible to apply the rules of differentiation learned in calculus by hand or programatically, but this could be time consuming or computationally difficult. The chain

rule, however, can be applied programatically and the function can be rewritten and deconstructed until a series of simple expressions remain for the program. From here, the derivative of each expression (W_i) can easily be determined and multiplied to form a new expression representing the exact derivative of the function in terms of each component (i.e. the gradient of $f(x, y)$). Two separate methods of automatic differentiation, known as the forward and reverse mode, are available. Forward mode allows for the derivative to be evaluated based on values of the input. It is named forward mode because it follows the natural progression in which expressions are typically evaluated. Specific parameters (x,y,z,...) can then be fed to the new expression and a continuous value of the derivative can be determined. If the goal is to determine the gradient of a parameter in terms of a large number of output functions, forward mode automatic differentiation is desired. If, however, there are a large number of input parameters and a few monitored output values (a common circumstance in catalysis), then reverse mode AD is desired. Reverse mode takes some output value and propagates information backwards to determine the gradient of the output value in terms of all parameters.

A more detailed discussion is beyond the scope of this work, but AD is implemented in FEniCS through the use of model adjoints that take advantage of the structure of the differential operators [48] . It is important to note that the derivatives found through automatic differentiation are exact and only limited by floating point errors. To achieve the accuracy of automatic differentiation, numerical differentiation requires a very small step size, which can often be difficult to achieve due to round-off error. On the other hand, using a step size that is too large results in inaccuracies in the value of the derivative due to the approximation. Further, it is necessary to remember that optimization requires the minimization of a function. The degree to which each of these parameters influences the value of this function is determined by the Jacobian. Accurate derivatives in the Jacobian are critical to the success of an optimization process.

5.2 Sensitivity Analysis Efficiency

To better understand the time requirement for performing a sensitivity analysis, as well as to gain insight into the time requirements for the evaluation of the Jacobian, a simple efficiency analysis was performed. Figure 15 shows how the time required to determine the sensitivity changes with the time step for two separate mechanisms. The first reaction mechanism (E.R./L.H.) is the combined Eley-Rideal/Langmuir-Hinshelwood model presented in section 4 and the second mechanism (E.R./L.H. w/A) is the same reaction with the addition of a simple, non-reactive adsorption process (A + * <-> A*). The plot shows an important efficiency challenge. Over the first time steps, the time required to determine the sensitivity of each parameter is on the order

of seconds. This rapidly increases to minutes and approaches hours per iteration over the course of the sensitivity analysis. The observed linear trend indicates that the addition of a time step results in a nearly fixed increase in the required time. This suggests that a sensitivity analysis should only be performed once all other parameters are set. With the current implementation, it seems the total amount of time required to perform a sensitivity can be determined as follows

$$\sum_{n=1}^{N_T} n \cdot t \tag{17}$$

where n is the iteration, N_T is the total number of iterations and t is the time required for each backward step in time. Though it is known t increases with the complexity of the equations, it is currently not known how to predict exactly how this value will scale.

Although the accuracy of the sensitivity analysis remains unparalleled by alternative methods, determining the sensitivity of each parameter is still costly. When the sensitivity is calculated at each time step, it must trace back to the beginning of the first time step during each calculation. It also takes approximately the same amount of time to calculate each sensitivity. This leads to a relatively inefficient, though thorough, evaluation of the sensitivity over time. Nonetheless, the time is still tractable in the context of computational catalysis, where DFT simulations can take days or weeks.

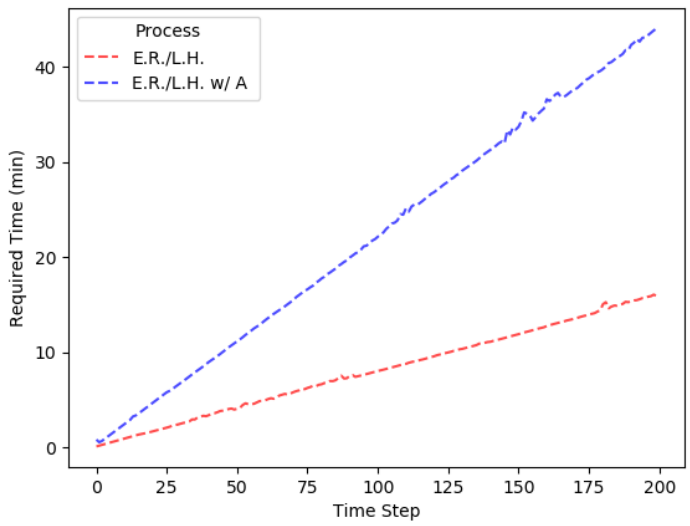

Figure 15: The time required to determine the sensitivity at each iteration of the sensitivity analysis. The two mechanisms investigated were an Eley-Rideal/Langmuir-Hinshelwood combination with and without the additional reversible adsorption of species A. Though E.R./L.H. process already took a significant amount of time per iteration, the time required is more than doubled when an additional adsorption process is included.

5.2.1 Application of the Sensitivity Analysis

A sensitivity analysis was performed on the carbon monoxide oxidation reaction mechanism with multiple reactive oxygen surface species, originally discussed and simulated in section 4. Figures 16 through 20 show the sensitivity of each gas (carbon monoxide and carbon dioxide) relative to each kinetic parameter. The pulsed inert does not interact with the catalyst material, so the inert was excluded from these figures. In each of these figures, ten separate curves are plotted for each gas species, representing all ten pulses introduced to the reactor during the experiment. The color of each curve indicates the pulse order of appearance, with purple and red showing the first and tenth pulses, respectively. A vertical color bar is included with each figure and indicates the color associated with each pulse. Each of the pulses in-between purple and red follows the associated color trend found on the color bar. The reaction and rate constant being monitored, as well as the line pattern used to represent each gas, are presented in the upper and lower right corners of each figure. To make the sensitivity analysis correspond to the degree of rate control analysis, and to normalize the curves, the sensitivity was multiplied by the rate constant and divided by the outlet flux at each time step for each gas species.

These figures show how influential each parameter is on each of the gasses outlet flux for the duration of the pulse. A positive value indicates an increase in the outlet flux from an increase in the kinetic parameter, while a negative value indicates a decrease in the outlet flux from an increase in the kinetic parameter. The extent to which these rate constants influence the outlet flux are not constant during the pulse and typically follow the standard TAP pulse curve. This should be expected, since the rate constant will be more influential in the presence of a higher gas concentration, i.e. around the peak of the pulse. This also leads to little insight being gained from the tail end of the pulse. Having an increase in kinetic parameters will result in a minimal shift in the outlet flux in the absence of reactants. Though these figures do follow general trends, unique features can be observed.

Figures 16 and 17 show the sensitivity of the gas species to the forward (Ke0) and reverse (Kd0) rate constants of carbon monoxide oxidation. As expected, increasing the forward rate constant will result in a reduced outlet flux of carbon monoxide, while an increase in the reverse rate constant will result in an increased outlet flux of carbon monoxide. The outlet flux of carbon dioxide is also impacted by shifting these parameters, but in an opposite manner.

The general shape of the sensitivity curves shown in Figure 20 are the most unique among the the sensitivity analyses for each parameter. Instead of having the traditional TAP pulse shape, the curve goes from a positive influence on the outlet flux at the start of the pulse and transitions to

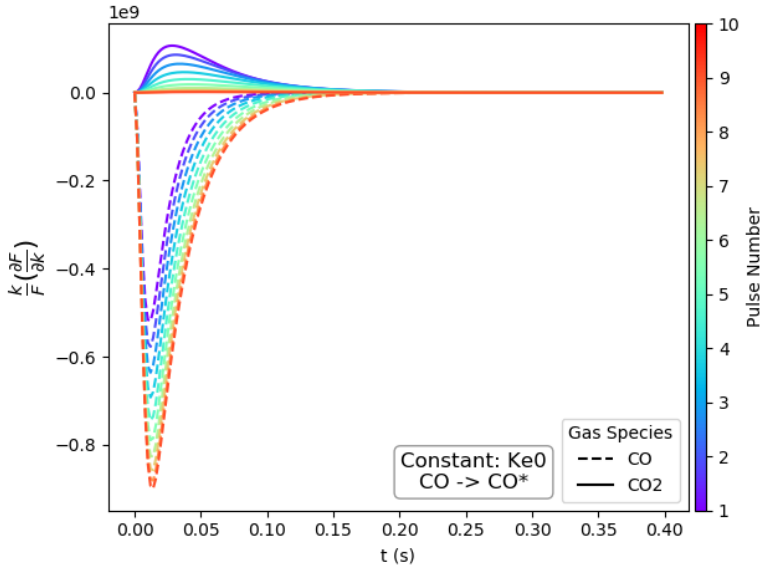

Figure 16: Sensitivity of carbon monoxide and carbon dioxide to the forward rate constant of the first elementary reaction (Ke0) over ten pulses.

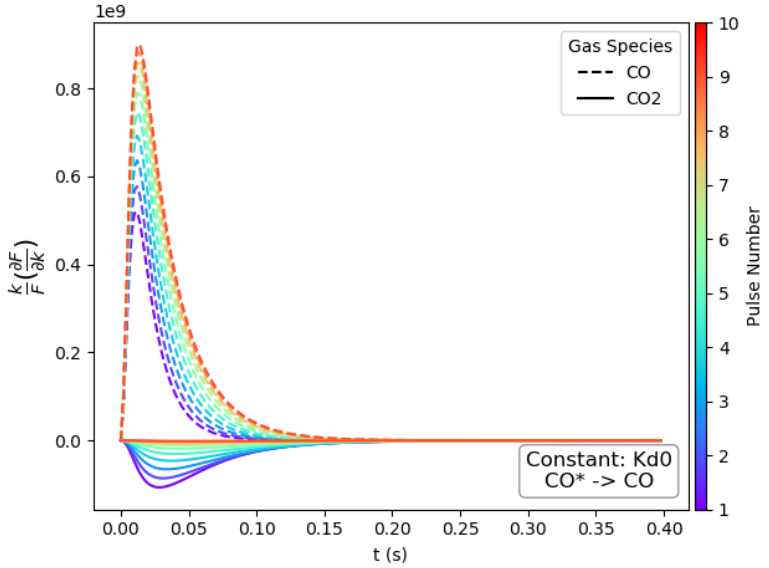

Figure 17: Sensitivity of carbon monoxide and carbon dioxide to the reverse rate constant of the first elementary reaction (Kd0) over ten pulses.

a negative influence around 0.03 seconds. This can be explained by the meaning of a higher rate constant for the duration of the pulse. If all the reactants are rapidly converted to the products and diffuse to the exit of the reactor, you will have less available for reaction and diffusion later. This results in a higher flux at the beginning of the pulse and a lower flux later.

Though computationally expensive, performing a Degree of Flux Control can provide unique kinetic insights about a catalyst. For more complex reactions, this method could help identify the rate limiting steps when they are less obvious during different stages of the pulse, similar to the

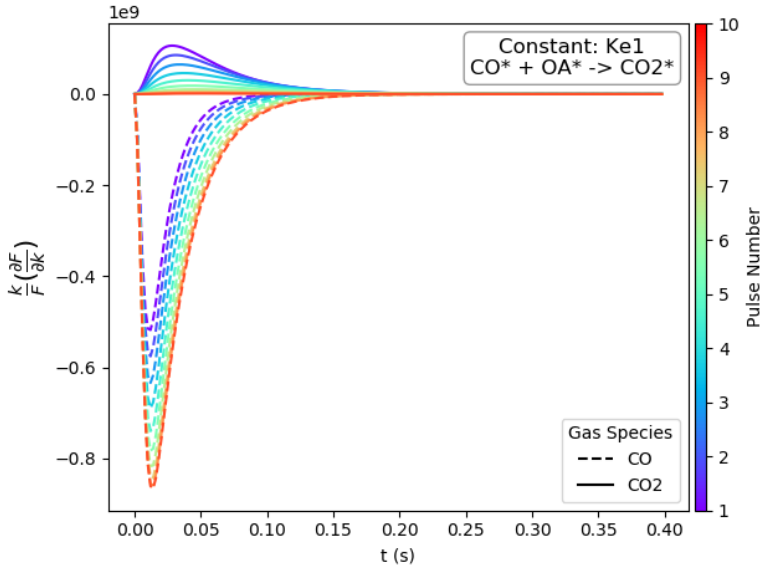

Figure 18: Sensitivity of carbon monoxide and carbon dioxide to the forward rate constant of the second elementary reaction (Ke1) over ten pulses.

traditional DRC. This application also highlights the accuracy of the derivatives generated from AD. It is unlikely that numerical differentiation would lead to derivatives of a similar stability. The computational burden could also be minimized by truncating the process and only calculating derivatives at early times when it is less expensive. Though improvements can be made, this is a useful addition to the TAP pulse processing workflow.

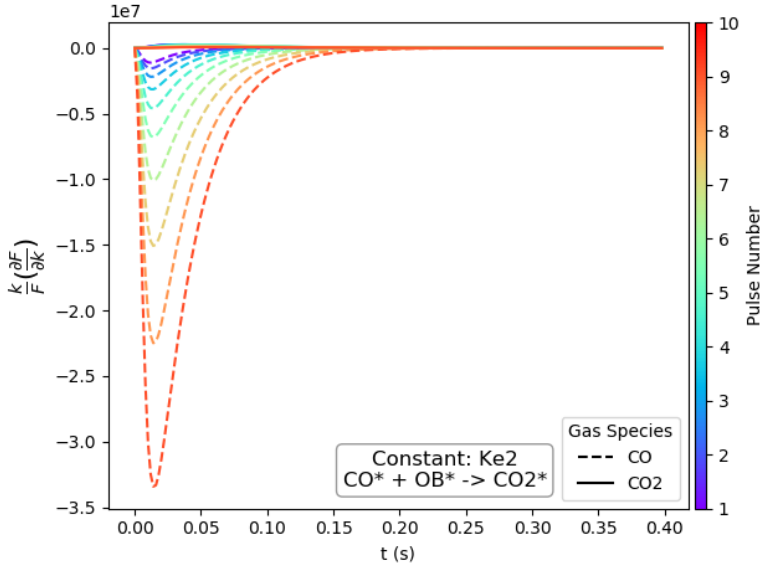

Figure 19: Sensitivity of carbon monoxide and carbon dioxide to the forward rate constant of the third elementary reaction (Ke2) over ten pulses.

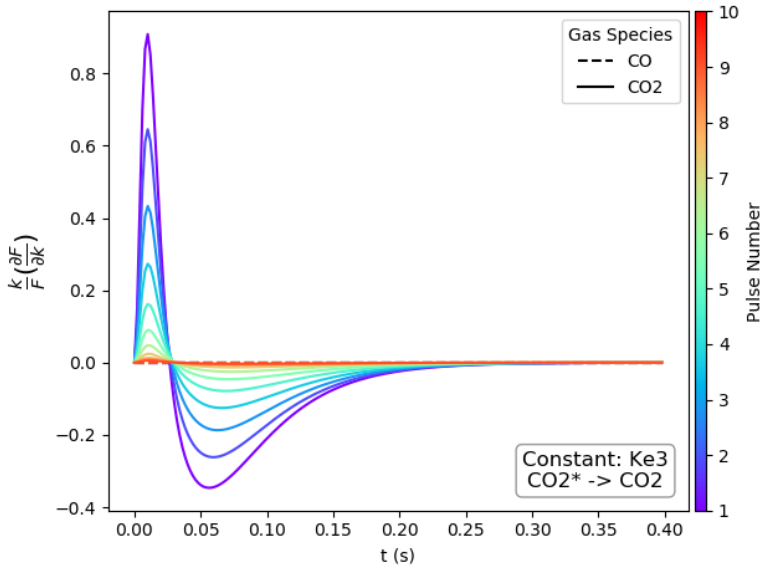

Figure 20: Sensitivity of carbon monoxide and carbon dioxide to the forward rate constant of the third elementary reaction (Ke3) over ten pulses.

6 Application of Parameter Fitting to TAP Models

A method to fit kinetic parameters to experimental data based on user defined reaction mechanisms has been developed. Some successful optimization methods for fitting kinetic parameters to TAP pulses have previously been developed and applied[76;77;78]. Of the applications, the most notable was performed by Kondratenko et al., who studied how well several different nitrogen oxide decomposition mechanisms fit to the experimental TAP data[79], with a mechanism proposed by Heyden et al. showing the strongest correlation[80]. The method implemented to fit parameters to these mechanisms was developed Wolf et al.[81;82;83]. Though it was able to successfully differentiate between mechanisms and fit parameters, it did struggle with efficiency and required strong initial guesses for the parameters to converge. More recent successful parameter regression methods have been implemented, including an application to the oxidative coupling of methanol over a nano-porous gold catalyst[84]. Though it did assist in understanding the mechanism, the regression method also required strong initial guesses from separate single crystal surface science experiments and fitting times ranged from hours to days. Requiring parameters from experimentation to fit parameters is a major limitation, especially when these experimental methods are not optional or the data is not available.

One underlying challenge in determining the kinetic parameters with these methods is the accuracy of the derivatives used during optimization. Wolf et al. specifically highlighted this struggle and noted that a "straightforward, although less efficient, gradientless method was used, since in the present problem the concentration of non-measurable surface species had to be calculated nu-

merically. This prevented any reliable use of gradient techniques which require precise values of derivatives of the differential equations."[81] This is where FEniCS and automatic differentiation is particularly useful, since the gradients generated through automatic differentiation have a much higher accuracy than traditional numerical differentiation methods[85]. In the following subsections, the parameter fitting method will be applied to the diffusion coefficients of multiple gasses, the kinetic parameters of a simple linear reaction, and several examples of carbon monoxide oxidation. The last carbon monoxide oxidation example will include a separate oxygen pulse to provide a more complex example. These examples will not only show the programs ability to fit parameters, but will also outline potential challenges and areas where improvement will be needed.

6.1 Fitting Parameters with FEniCS

To fit parameters to experimental data, it is required to define an objective to be minimized. Proper definition of the objective function can be crucial in optimization, as noted by Savara et al[86]. In the case of TAP reactors, the objective function (N_T) is defined as follows

$$J = \sum_i (\frac{1}{2} \int_{L-\triangle x}^{L} |u_i(x,t) - u_{i,obs}(x,t)|^2 dx) \tag{18}$$

where i represents each of the points considered, L is the length of the reactor, u_i is the concentration profile of the forward solution, $u_{i,obs}$ is the experimental data, and $\triangle x$ is the mesh step size. The inner product is evaluated over the spatial step at the reactor outlet, i.e. $L - \triangle x$ to L. The objective function consists of a series of inner products between the data points and the outlet concentration of the FEniCS simulation. During the forward simulation, when an experimental data point is needed for a specific gas, an objective function will be defined, assembled and added to the final objective function. Since calculating the gradient for all data points can be time intensive, it is not recommended for the user to define their objective function over all the data points generated. Instead, it is suggested that the number of points be reduced with a few potential options.

First, an objective function can be defined at the peak of each of the gas species curves. The program will automatically locate this peak in the data for each gaseous species and store its associated time. Second, five points can be distributed over the curve to define the objective function. One way to do this would be to again use the peak as a point, but also include two points before and after the peak. The two points to the left of the peak would be at the first time step and also at the halfway point between the initial point and the peak. The two points to the

right of the peak would be located at 50% and 20% of the peak height. The choice of five points can be thought of as a net draped over the data, where the fundamental shape of each outlet curve can be captured without specifying all points. Last, the objective function could be modified to involve all points in the experimental data before the pulse curve reaches a negligible size (i.e. becomes flat). For more complex reaction networks, the use of all reaction points could be used.

For all of these methods, it is important to keep in mind the time required to calculate the jacobian. Looking back at figure 15, it can be noted that the further along the simulation is, the more time it takes to determine the derivatives. This means that there is a significant difference between the cost of the derivative for the points occurring before the peak and those following it. So having a larger number of points before the peak and including only a couple after could also be the optimal circumstance for fitting these parameters.

Though the objective function and Jacobian are evaluated with FEniCS, the optimization is performed through Scipy. Currently, the Limited-memory Broyden-Fletcher-Goldfarb-Shanno (L-BFGS) optimization method, which is the default in FEniCS, is used. Other methods could be tested for efficiency and accuracy improvements, but a proof of concept is the current motivation. Parameter estimation is included in the functionality of the simulator. The location of the experimental data can be specified with the user input file. Currently, the number of data points must match the number of time steps exactly. This could be a challenge going forward, since the values could vary significantly. In future implementations, if a desired point for fitting is not exactly determined in the simulator, can be used for interpolation to obtain a value as close as possible to the desired point. Further, this data does not include noise, which will always be present in experimental data. Testing the programs ability to fit parameters to noisy experimental data, as well as developing methods to reduce this noise, will be the subject of future studies. Currently, simple boundaries are applied to the optimization method (i.e. rate constants or diffusion coefficients cannot be negative). Stronger bounds will likely be necessary for fitting more complex reaction equations in future implementations.

6.2 Diffusion Coefficients

Before applying the parameter fitting method to kinetic parameters, the diffusion coefficients for multiple gases were simultaneously fit to test the implementation. Figure 21 shows the steps taken through the minimization process to arrive at the correct diffusion coefficients. Since the diffusion coefficients used in TAP reactors are often defined through Grahams law of diffusion, the values presented in the figure are the masses of each species. The initial guess for the mass of each

species was four-hundred (an intentionally poor guess for the visualization of the method), while the actual masses were 10, 50 and 100 for gaseous species A, B and the inert, respectively. This showed that multiple parameters could simultaneously be fit with the defined objective function and optimization method. The parameter fitting method is able to accurately determine the masses of each of the gaseous species with only a single point for each gas species being specified in the objective function. Though it was successful with a single point, future methods will likely require multiple points on the curve, even if it is desired to fit the diffusion coefficients alone due to noisy data. At the moment, noise free data is used in place of true experimental data, but methods exist for adding noise and this will be a challenge for future work.

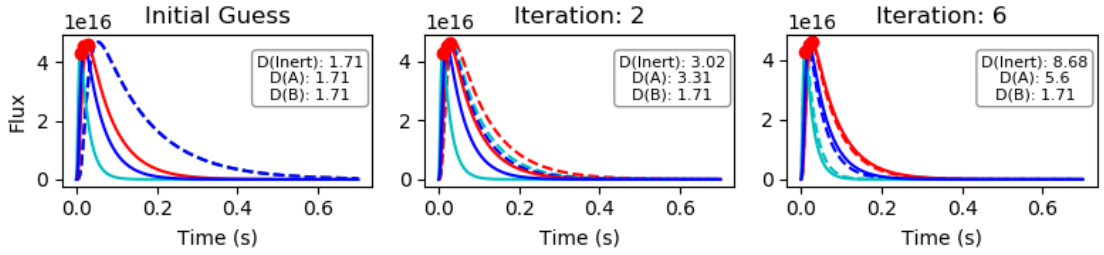

Figure 21: The simultaneous fitting of diffusion coefficients for three separate gas species, with the solid lines representing the experimental data provided by the user and the dashed lines representing curves during each iteration. The same initial guess was made for all three gases (left panel). The parameters are nearly converged by the sixth iteration (right panel). To reduce the computational burden on minimizing the objective function, the curves were only fit to the red peaks.

6.3 Linear Reaction Model

Though useful for validation, the Knudsen diffusion coefficients will typically be known for the gases studied through the application of Graham's Law, and will not require parameter fitting. To test the parameter fitting method on a more challenging system, while avoiding non-linear models, the parameters of the linear reaction mechanism introduced in section 3.4 were fit. This mechanism involves two reactions: the adsorption of species A and the desorption of adsorbed A as species B. Figure 22 shows the steps the optimization method took to determine the parameters. Initially, the program takes multiple steps in altering the second rate constant. Once the curve representing B was close to the experimental result, the optimization method began making larger changes to the first rate constant. This resulted in a decrease in the size of curve A, but also an increase in the size of curve B. After a few iterations with decreases in A and increases in B, both curves began to converge to the exact solution with accurate kinetic parameters. The fitting of parameters to this linear model also took more iterations than the previous diffusion example. This is likely due to the challenge of fitting two curves that are related to each other through the reaction expressions. Initial changes to the second rate constant, responsible for producing B, will initially have little

impact on the minimization of the objective function. This is due to the initial guesses (which were zero) and the lack of A present on the surface, which will lead to a limited change (i.e. insensitive to this parameter) in the curve for B.

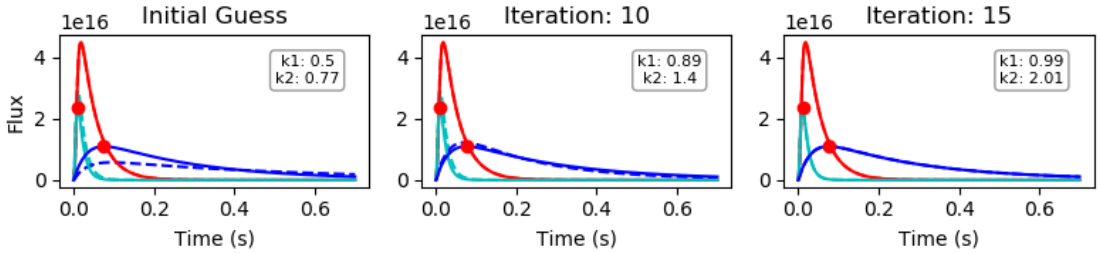

Figure 22: The fitting of two forward rate constants for a simple linear reaction mechanism (presented in section 3.4). Though a straight forward implementation, it does show that it is possible to determine the kinetic parameters of a reaction mechanism with the current implementation

6.4 Carbon Monoxide Oxidation

6.4.1 Eley-Rideal / Langmuir-Hinshelwood Parameter Fitting to Carbon Monoxide Oxidation Synthetic Data

The parameters of Eley-Rideal and Langmuir-Hinshelwood reaction mechanisms were fit to two sets of synthetic data, generated from the mechanisms being fit. These were both relatively simple reaction mechanisms, involving only one or two elementary reactions. This offers an opportunity not available in the previous two examples: testing the fit of two separate mechanisms on the same set of experimental data to see if a conclusion can be drawn about the actual mechanism.

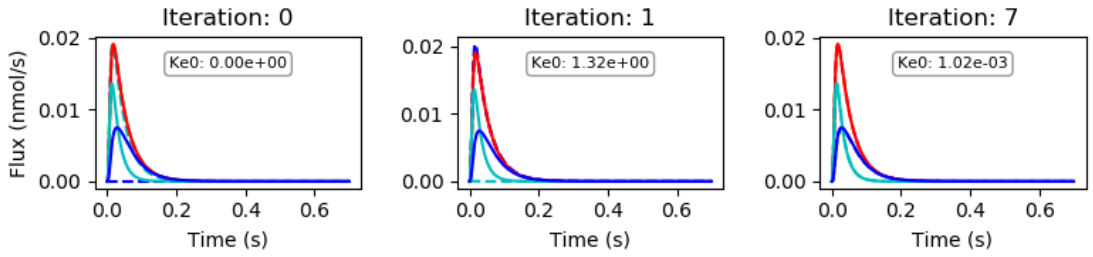

Figure 23: Fitting an Eley-Rideal carbon monoxide oxidation reaction mechanism to synthetic data generated from the same Eley-Rideal mechanism. The actual rate constant (Ke0) was set to 1e-3. The bold and dashed lines represent the synthetic and experimental data, respectively, with carbon monoxide, carbon dioxide and the inert appearing in cyan, blue and red.

First, the Eley-Rideal mechanism was fit to the synthetic Eley-Rideal and Langmuir-Hinshelwood data. Figures 23 and 24 show the steps taken by each mechanism to arrive at their respective solutions. Similar to the linear model fitting process, an initial guess of zero was used for each. The initial step taken by the process over shoots the value of the forward rate constant, resulting in a

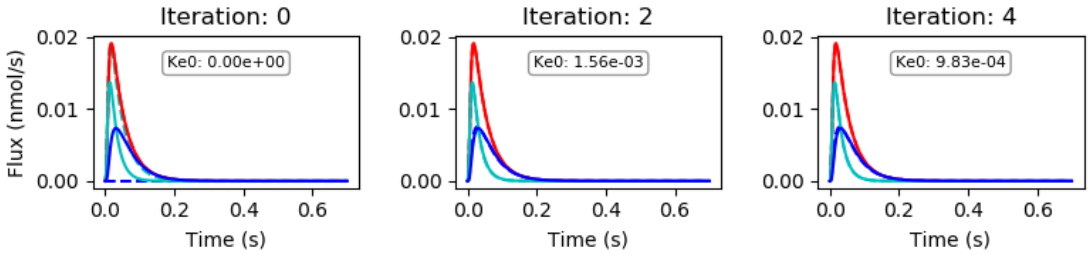

Figure 24: Fitting an Eley-Rideal carbon monoxide oxidation reaction mechanism to synthetic data generated from a Langmuir-Hinshelwood mechanism. The forward (Ke0) and reverse (Kd0) rate constants were set to 1e-3 and 10, while the desorption rate constant (Ke2) of carbon dioxide was set to 1e-3. The bold and dashed lines represent the synthetic and experimental data, respectively, with carbon monoxide, carbon dioxide and the inert appearing in cyan, blue and red.

nearly zero value for the carbon monoxide curve and a carbon dioxide curve resembling the size of the inert curve. After approximately seven iterations, the rate constant is able to converge to a value close to the correct answer, 1e-3. Fitting the Eley-Rideal mechanism to the Langmuir-Hinshelwood data was less successful. The mild elongation of the carbon monoxide curve is unable to be matched when fitting the Eley-Rideal mechanism. This gives some indication that a mechanism can be identified if an attempt to fit a simple mechanism to a complex mechanism is made. This could also mean that trying to observe the correct mechanism could rely on trying to fit the simplest mechanism first.

Second, synthetic data for the Langmuir-Hinshelwood reaction mechanism was generated and the Eley-Rideal and Langmuir-Hinshelwood mechanisms were fit. Figures 25 and 26 show the steps taken by each mechanism to arrive at their respective solutions. When fitting to the L.H. mechanism, the reverse rate constant was not determined and little change was observed between the iterations. This could be an indication that the constant is not sensitive to the objective function or it could be a sign that not all parameters can be determined using the current method. Five points were also used to fit kinetic parameters to the Langmuir-Hinshelwood reaction mechanism based on each set of synthetic data, too, and are presented in figures 27 and 28. Though the number of iterations was lower compared to the single point fitting method, each iteration did take longer. With this added information from multiple pulses, the parameters were found to fit no better and no immediate conclusion about the validity of the mechanism could be made. One notable change between the single point and five point objective function implementations was observed when fitting to the E.R. mechanism. The values of the rate constants appear to converge to a value that would indicate the E.R. mechanism. The forward rate constant for carbon dioxide formation becomes relatively large, indicating an instantaneous desorption of the carbon dioxide formed, while the forward rate constant for the adsorption of carbon monoxide converges to the correct value. In a way, this shows that additional points are identifying the correct mechanism

even though it is over fitting the parameters. But expanding the program to make these types of conclusions automatically is not currently implemented.

Based on these example, the appropriate choice of mechanism was not able to be determined strictly through parameter fitting, but certain 'fingerprints' were observed. Since an Eley-Rideal reaction mechanism results in the direct formation of carbon-dioxide from carbon monoxide, an elongation of the carbon dioxide curve will not be observed from this mechanism. Previous applications of parameter fitting have fit mechanisms in order of complexity, beginning with the simplest and concluding with the most complex. It was also shown that the use of a single point is not always acceptable for fitting parameters.

It also shows that using a single point for optimization can lead to an inaccurate simulation curve. The need for the transient data generated from TAP experiments is justified. A single point for each curve in the objective function will not necessarily lead to the synthetic and TAP curves matching exactly. This does not mean that all data points will be necessary though. As noted in section 5, this would lead to a burdensome computational expense and time requirement. For this reason, a set of points could balance the time intensity with the kinetic information.

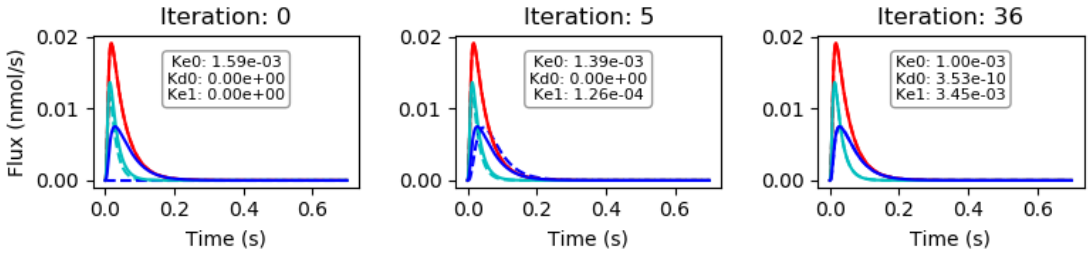

Figure 25: Fitting a Langmuir-Hinshelwood carbon monoxide oxidation reaction mechanism to synthetic data generated from an Eley-Rideal mechanism. The actual rate constant (Ke0) was set to 1e-3. The bold and dashed lines represent the synthetic and experimental data, respectively, with carbon monoxide, carbon dioxide and the inert appearing in cyan, blue and red.

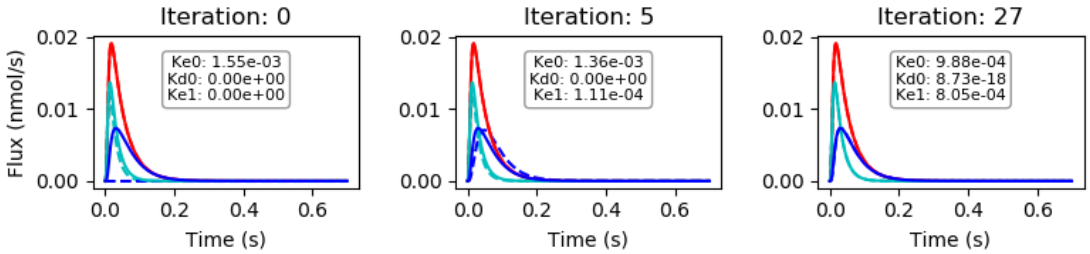

Figure 26: Fitting a Langmuir-Hinshelwood carbon monoxide oxidation reaction mechanism to synthetic data generated from the same Langmuir-Hinshelwood mechanism. The forward (Ke0) and reverse (Kd0) rate constants were set to 1e-3 and 10, while the desorption rate constant (Ke2) of carbon dioxide was set to 1e-3. The bold and dashed lines represent the synthetic and experimental data, respectively, with carbon monoxide, carbon dioxide and the inert appearing in cyan, blue and red.

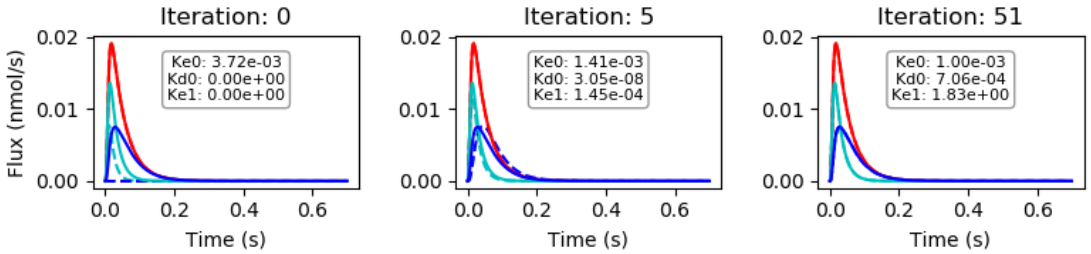

Figure 27: Fitting a Langmuir-Hinshelwood carbon monoxide oxidation reaction mechanism to synthetic data generated from an Eley-Rideal mechanism with five Points. The actual rate constant (Ke0) was set to 1e-3. The bold and dashed lines represent the synthetic and experimental data, respectively, with carbon monoxide, carbon dioxide and the inert appearing in cyan, blue and red.

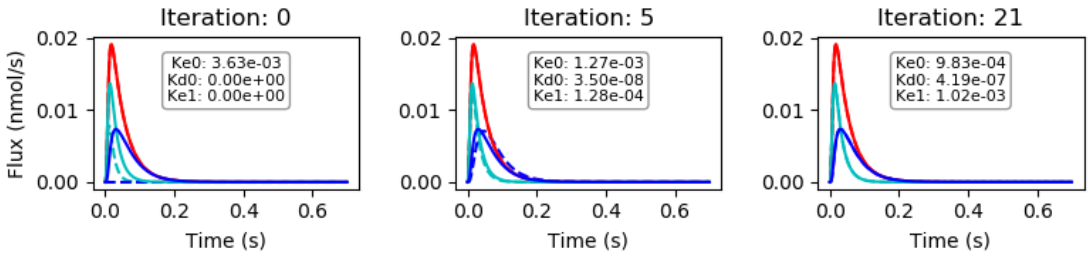

Figure 28: Fitting a Langmuir-Hinshelwood carbon monoxide oxidation reaction mechanism to synthetic data generated from the same Langmuir-Hinshelwood mechanism with five Points. The forward (Ke0) and reverse (Kd0) rate constants were set to 1e-3 and 10, while the desorption rate constant (Ke2) of carbon dioxide was set to 1e-3. The bold and dashed lines represent the synthetic and experimental data, respectively, with carbon monoxide, carbon dioxide and the inert appearing in cyan, blue and red.

6.4.2 Fitting Parameters to Synthetic Data with Multiple Reactant Feeds

Applications of the parameter fitting in previous sections showed a steady increase in the complexity of the reaction network, from no reactions (diffusion) to a couple elementary reactions (Langmuir-Hinshelwood mechanism). The complexity of the equations can be further expanded through the inclusion of an additional gas reactant in the Langmuir-Hinshelwood carbon monoxide oxidation mechanism, O_2. The equations used in this simulation are as follows:

$$CO + * \leftrightarrow CO^* \tag{19}$$

$$O_2 + 2* \leftrightarrow 2O^* \tag{20}$$

$$CO^* + O^* \rightarrow CO_2 + * \tag{21}$$

The results of fitting parameters using the five-point method from the previous sections are presented in figure 29. Though the curve representing carbon monoxide adsorption shows a strong overlap, a clear difference between the experimental and simulated oxygen curves is noticeable.

Further, the simulated curve representing carbon dioxide does not appear at all.

Attempting to fit the parameters to this reaction network presented a major challenge and showed that a direct method to fit all kinetic parameters will not always work. It appears that the objective function reaches a local minima with each of the curves representing reactant gases matching their respective experimental curves relatively well. Though the curve representing the product gas in no way resembles the associated experimental curve, changing the parameters results in a greater increase in the difference between the reactant gases than a greater reduction in the difference between the product curves. This is a major flaw in the parameter fitting process and would limit the parameter fitting method to simple sets of elementary reactions or to adsorption processes. Two potential solutions exist to overcome this challenge. First, the products could be pulsed independently of the reactants. This method could have trouble when the adsorption and subsequent reaction of the product gasses are unfavorable. This leads to the second option, where better initial guesses are provided. One pragmatic approach to accomplish this would be defining the objective function to exclusively include the product pulse curves. The parameters found from the initial, failed optimization can be used as an initial guess for the new objective function. Once this second optimization process is complete, the new parameters can be fed to the original optimization problem and run to completion.

The redefinition of the objective function to only include the product curve is presented in figure 30. This second optimization process shows that there is now a change to the carbon dioxide curve even though it results in a change to the other reactant curves. The objective function was then again redefined to include all curves and is presented in figure 31. Though it is not able to converge to the exact solutions, it is a dramatic improvement from the original optimization method, where only the initial kinetic parameters are able to be determined.

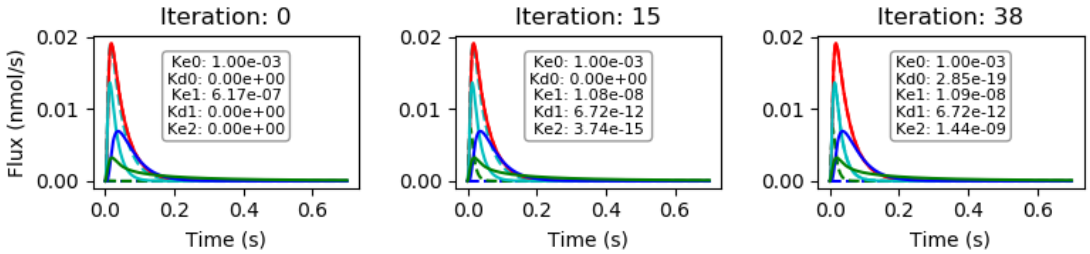

Figure 29: The initial attempt at fitting kinetic parameters to synthetic data carbon monoxide oxidation involving gaseous oxygen, with carbon monoxide, carbon dioxide, oxygen and the inert appearing in cyan, blue, green and red. The actual rate constant (Ke0) was set to 1e-3. The bold and dashed lines represent the synthetic and experimental data, respectively, with carbon monoxide, carbon dioxide and the inert appearing in cyan, blue and red.

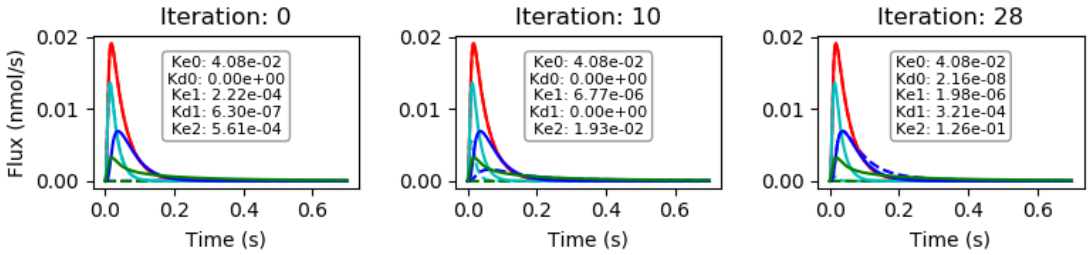

Figure 30: The second attempt at fitting kinetic parameters to synthetic data carbon monoxide oxidation involving gaseous oxygen, with carbon monoxide, carbon dioxide, oxygen and the inert appearing in cyan, blue, green and red. For this attempt, the results of the previous attempt at fitting the parameters were used as initial guesses and the objective function was redefined to include only carbon dioxide.

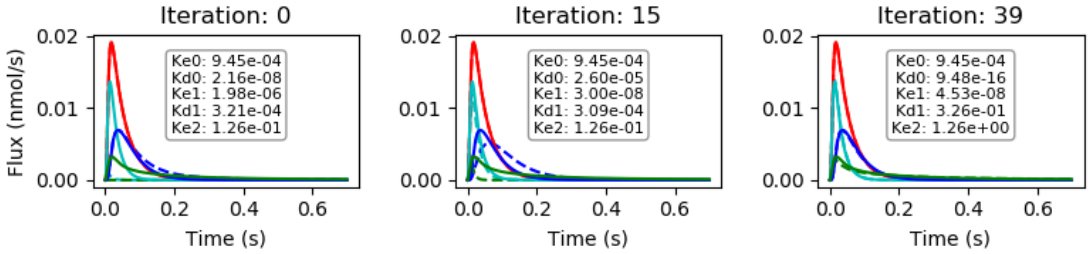

Figure 31: The third attempt at fitting kinetic parameters to synthetic data carbon monoxide oxidation involving gaseous oxygen, with carbon monoxide, carbon dioxide, oxygen and the inert appearing in cyan, blue, green and red. For this attempt, the results of the second attempt at fitting the parameters were used as initial guesses and the objective function was redefined to include all species again.

7 Future Work

7.1 Establishing Boundaries and Initial Guesses for Parameter Fitting and Mechanism Identification

Though the use of AD does not require strong initial guesses like traditional parameter fitting methods, having them could make the process more efficient. Similarly, having boundaries on kinetic parameters could help lead the user to correct physical conclusions. There are many options for making initial guesses and setting bounds, but two methods stand out in particular.

First, the results from DFT calculations and surface science experiments can be used. Intrinsic kinetic parameters are often presented in the literature involving these two methods. Though there is a chance that the experiments were performed previously, there are many existing materials and catalyst states that have not been previously studied. If feasible, these experiments can be performed by the investigators. This is a non-ideal circumstance and will lead to longer, costly experiments and would require a broader skill set and equipment availability. A cheaper way to arrive at initial guesses would be to apply the scaling relations developed using DFT, although the accuracy of these tools can be limited and do not necessarily translate between active sites or catalysts.

Second, the Y-Procedure and RRM could be used to establish new guesses. Before this can be implemented in the workflow, a proper understanding of the results of the Rate-Reactivity Model must be established. Limited implementations of these methods have been made and confirmation of their accuracy must still be made. It was proposed that the coefficient fit in this linear model represents the Jacobian of the reaction mechanism. If true, this could be implemented in an automatic way to generate new, cheap initial guesses.

For this reason, the first steps in validating this process have been taken and a proposed workflow has been developed (see Figure 32). Generating visual comparisons of the Jacobian could help identify where each correlate or deviate. This is a convenient circumstance, since a method to simulate a reaction based on a system of elementary reactions (an MKM) has been developed and methods of post processing the data and generating symbolic derivatives of the MKM can easily be incorporated into the workflow. There are many options available for establishing estimates and boundaries that could be implemented automatically, but testing and validating these methods must still be completed.

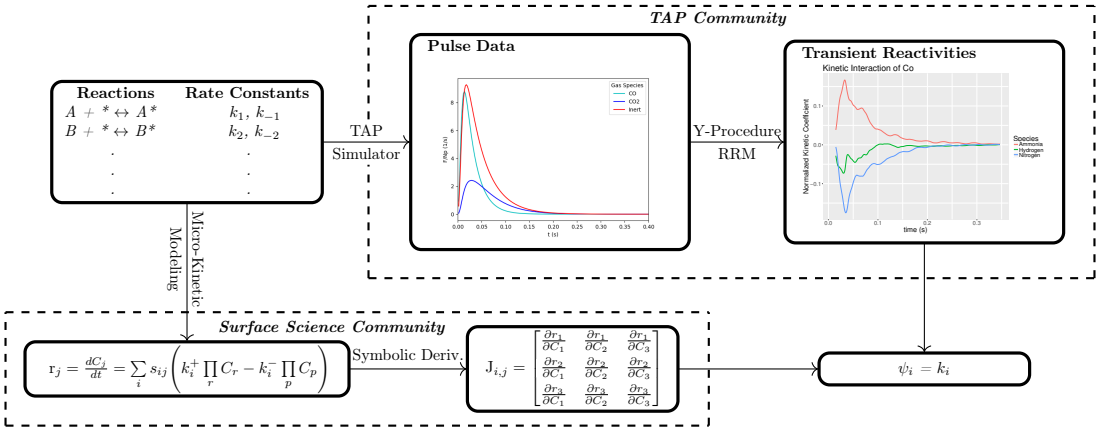

Figure 32: Simultaneously performing an analysis of synthetic pulse data with the Rate-Reactivity Model and Derivatives from Automatic Differentiation could help elucidate to meaning of the Reactivates found from the RRM. Having this meaning could lead to cheap initial guesses for the parameter fitting method.

7.2 Application of the Simulation Package to Complex Reactions and Surfaces

It will also be important going forward to apply TAP and its associated analysis tools to more complicated reactions and surfaces. Carbon monoxide oxidation is an appropriate probe reaction for validation, but does not confirm the utility of the process for more complicated mechanisms. Ammonia decomposition is an appropriate mechanism to investigate next because it offers a complex, albeit bounded, reaction mechanism. If diazene and hydrazine are not present in the outlet flux, then the reaction mechanism will only consist of the adsorption of ammonia and subsequent cleavage of each of its hydrogen atoms, followed by the desorption of hydrogen and nitrogen gas.

$$NH_3 + * \leftrightarrow NH_3^* \tag{22}$$

$$H_2 + 2* \leftrightarrow 2H^* \tag{23}$$

$$N_2 + * \leftrightarrow N_2^* \tag{24}$$

$$N_2* \leftrightarrow 2N^* \tag{25}$$

$$NH_3^* \leftrightarrow NH_2^* + H^* \tag{26}$$

$$NH_2^* \leftrightarrow NH^* + H^* \tag{27}$$

$$NH^* \leftrightarrow N^* + H^* \tag{28}$$

Further, investigating reaction mechanisms on complex surfaces is desired. Mixed metal oxides

are of particular interest because their diverse mixture of atoms can lead to many potential active sites[87;88;89;90]. TAP reactors could help elucidate some of the intrinsic kinetics and help reduce the number of potential solutions to the mechanism.

7.3 Improving the Sensitivity Analysis and Parameter Fitting Efficiency

Being able to evaluate the derivatives over time is a necessary step for both the sensitivity analysis and parameter fitting tools. At the moment, it takes a considerable amount of time to determine these derivatives and will act as a bottleneck in analyzing TAP pulses. Reaction mechanisms can easily involve a dozen elementary reactions, which is a challenging problem for parameter fitting. Testing multiple reaction mechanisms over hundreds of pulses is an additional data intensity challenge. Since it is desired to apply the simulator and parameter fitting method to this scale, the efficiency will have to be improved. The time required per simulation could be reduced with an adaptive time stepping algorithm. Performing the Degree of Flux Control is also a time intensive process and could be improved with algorithms designed for transient sensitivity analysis. Improvements and developments to FEniCS and Dolfin-Adjoint can easily be swapped for current called functions in the script due to the way the scripts were written.

7.4 Application of FEniCS to Other Reactor Models and Inclusion in CATMAP

The tools developed thus far could be applied to other, more common reactors used in academia and industry, too[91;92]. The modeling, sensitivity analysis and parameter fitting possible in the TAP reactor simulator could be useful to any catalysis based group if further generalized and could act as a replacement or alternative to the methods commonly used[93;94;95;96]. By redefining the boundary conditions and transport properties in the equation generator, it is possible to model more traditional reactors and apply similar methods of analysis. For experimentalists, steps have already been taken to model simple transient and steady-state Plug Flow Reactors (PFRs), but confirming the accuracy of these models is still necessary. For computational groups, generalization of the simulator could be applied to the analysis micro-kinetic models. Applications of these new methods could reach even farther in the chemical engineering field and help generalize simulations in the separations[97;98;99;100] and electrochemistry[101;102] communities. A generalized version of the current FEniCS simulator would be a useful, natural progression from CatMAPs current form. Developing an open source package where dimensional reduction of catalysts can easily be feed to any desired reactor without user derivation is currently unavailable in the field. It is our goal

to incorporate a further generalized form of the package with CatMap[103], which could lead to powerful, broadly applicable tool for catalyst development and optimization[87;104].

8 Conclusion

TAP, with its high data intensity and ability to provide insight into complex, transient processes, has the potential to assist computational chemists, surface scientists and industrial catalyst experimentalists in gaining fundamental knowledge about materials of interest and testing their own proposed hypotheses about mechanisms and kinetic parameters. Before this is possible, methods to efficiently handle the data must be established. In this thesis, a foundation, consisting of four major components, has been developed, on which more elaborate data analysis methods can be built. Some of these methods have been implemented previously, but automatic differentiation has never been incorporated and most of the components are not publicly available. The most direct way to implement AD into TAP simulations is through the use of FEniCS.

A Python package for simulating TAP pulses and new methods to process these pulses have been developed. Though simulators have previously been implemented, they have been limited in their flexibility, as well as in their broader availability and utility. The application of FEniCS to this field is a significant milestone for many reasons. First, it is open source, unlike Maple or Matlab, meaning a software licence does not have to be purchased for use. Second, it allows users to easily apply automatic differentiation, which allows for the accurate evaluation of derivatives. The availability of accurate derivatives can help provide a meaningful sensitivity analysis and parameter fitting. And last, it is a young, developing package with an expanding community of contributors and developers, meaning improvements to the current, already useful programs will be made.

A simple csv input file was developed to make using the simulator less challenging for users with limited python experience, as well as to help keep track of the conditions used during each simulation. Validation of the simulator was performed by directly comparing the curves generated with the FEniCS simulator to curves generated from the analytical solutions and Maple simulator developed by other groups in the TAP community. The efficiency of the forward simulator was also tested and analyzed. The influence of mesh size, number of time steps and complexity of the reaction mechanisms were all probed. The package was applied to carbon monoxide oxidation, which is a common probe reaction because of its diverse, albeit limited, set of potential reaction mechanisms.

In addition, a method to generate previously unspecified reaction mechanisms was developed. This script takes in a set of elementary reactions and converts them to the appropriate PDEs to be used by FEniCS. Although not implemented in the workflow, methods to generate simple reaction mechanisms based on user defined reactants and products was developed, as well as a method to generate sets of rate expressions based on rate-limiting step approximations. These will provide

users with useful methods to explore the reaction kinetics of TAP pulses in future implementations.

Alongside the forward simulation, the package is designed to solve the inverse problems needed for sensitivity analysis and parameter fitting. The efficiency of performing a sensitivity analysis, which can be described as a transient form of Dr. Campbell's DRC, here called the Degree of Flux Control, was tested for two reaction systems. This Degree of Flux Control was also applied to a carbon monoxide oxidation reaction and helped identify interesting kinetic details. Each sensitivity analysis was found to be time intensive, indicating that calculating the Jacobian for an objective function involving all data points is currently computationally expensive. A method to fit parameters was also established and applied to several reaction mechanisms, including purely diffusive processes and simple linear reactions. The method was able to accurately determine the parameters for each of these test cases. This parameter fitting method was also applied to carbon monoxide oxidation simulations. Currently, the parameter fitting method is unable to differentiate between synthetic data generated from an Eley-Rideal or Langmuir-Hinshelwood reaction mechanism. When applied to a multi-reactant feed pulse, the fitting method struggled and converged to local minima. A potential method to handle this problem was tested and discussed, showing potential to reach the kinetic parameters through a series of optimization processes.

References

[1] I. Chorkendorff and J. W. Niemantsverdriet, *Concepts of modern catalysis and kinetics*. John Wiley & Sons, 2017.

[2] A. J. Medford, M. R. Kunz, S. M. Ewing, T. Borders, and R. R. Fushimi, "Extracting knowledge from data through catalysis informatics," *ACS Catalysis*, 2018.

[3] S. Cao, J. R. Monnier, C. T. Williams, W. Diao, and J. R. Regalbuto, "Rational nanoparticle synthesis to determine the effects of size, support, and k dopant on ru activity for levulinic acid hydrogenation to γ-valerolactone," *Journal of Catalysis*, vol. 326, pp. 69–81, 2015.

[4] R. P. Galhenage, H. Yan, A. S. Ahsen, O. Ozturk, and D. A. Chen, "Understanding the growth and chemical activity of co–pt bimetallic clusters on tio2 (110): Co adsorption and methanol reaction," *The Journal of Physical Chemistry C*, vol. 118, no. 31, pp. 17773–17786, 2014.

[5] R. Jinnouchi and R. Asahi, "Predicting catalytic activity of nanoparticles by a dft-aided machine-learning algorithm," *The journal of physical chemistry letters*, vol. 8, no. 17, pp. 4279–4283, 2017.

[6] R. Jinnouchi, H. Hirata, and R. Asahi, "Extrapolating energetics on clusters and single-crystal surfaces to nanoparticles by machine-learning scheme," *The Journal of Physical Chemistry C*, vol. 121, no. 47, pp. 26397–26405, 2017.

[7] M. Saleheen and A. Heyden, "Liquid-phase modeling in heterogeneous catalysis," 2018.

[8] A. J. Medford and M. C. Hatzell, "Photon-driven nitrogen fixation: current progress, thermodynamic considerations, and future outlook," *ACS Catalysis*, vol. 7, no. 4, pp. 2624–2643, 2017.

[9] B. M. Comer and A. J. Medford, "Analysis of photocatalytic nitrogen fixation on rutile tio2(110)," *ACS Sustainable Chemistry & Engineering*, vol. 6, no. 4, pp. 4648–4660, 2018.

[10] E. J. Houdry, M. R. Eriksson, and M. A. Coudray, "Gas treating apparatus," Aug. 4 1959. US Patent 2,898,202.

[11] W. Kohn, A. D. Becke, and R. G. Parr, "Density functional theory of electronic structure," *The Journal of Physical Chemistry*, vol. 100, no. 31, pp. 12974–12980, 1996.

[12] K. J. Laidler and M. C. King, "Development of transition-state theory," *The Journal of physical chemistry*, vol. 87, no. 15, pp. 2657–2664, 1983.

[13] J. Dumesic, D. Rudd, L. Aparicio, J. Rekoske, and A. Trevino, "The microkinetics of heterogeneous catalysis. 1993," *ACS Profesional Reference Book*.

[14] O. Mamun, "Theoretical investigation of the catalytic hydrodeoxygenation of levulinic acid over ru (0001) catalyst surface," 2017.

[15] N. Nikbin, P. T. Do, S. Caratzoulas, R. F. Lobo, P. J. Dauenhauer, and D. G. Vlachos, "A dft study of the acid-catalyzed conversion of 2, 5-dimethylfuran and ethylene to p-xylene," *Journal of catalysis*, vol. 297, pp. 35–43, 2013.

[16] P. Tereshchuk, A. S. Chaves, and J. L. Da Silva, "Glycerol adsorption on platinum surfaces: A density functional theory investigation with van der waals corrections," *The Journal of Physical Chemistry C*, vol. 118, no. 28, pp. 15251–15259, 2014.

[17] D. Coll, F. Delbecq, Y. Aray, and P. Sautet, "Stability of intermediates in the glycerol hydrogenolysis on transition metal catalysts from first principles," *Physical Chemistry Chemical Physics*, vol. 13, no. 4, pp. 1448–1456, 2011.

[18] P. Broqvist, I. Panas, and H. Persson, "A dft study on co oxidation over co3o4," *Journal of Catalysis*, vol. 210, no. 1, pp. 198–206, 2002.

[19] R. Watwe, B. Spiewak, R. Cortright, and J. Dumesic, "Density functional theory (dft) and microcalorimetric investigations of co adsorption on pt clusters," *Catalysis letters*, vol. 51, no. 3-4, pp. 139–147, 1998.

[20] J. Zaffran, C. Michel, F. Delbecq, and P. Sautet, "Trade-off between accuracy and universality in linear energy relations for alcohol dehydrogenation on transition metals," *The Journal of Physical Chemistry C*, vol. 119, no. 23, pp. 12988–12998, 2015.

[21] Y. Chen, M. Salciccioli, and D. Vlachos, "An efficient reaction pathway search method applied to the decomposition of glycerol on platinum," *The Journal of Physical Chemistry C*, vol. 115, no. 38, pp. 18707–18720, 2011.

[22] T. Bligaard, J. K. Nørskov, S. Dahl, J. Matthiesen, C. H. Christensen, and J. Sehested, "The brønsted–evans–polanyi relation and the volcano curve in heterogeneous catalysis," *Journal of Catalysis*, vol. 224, no. 1, pp. 206–217, 2004.

[23] J. K. Nørskov, T. Bligaard, J. Rossmeisl, and C. H. Christensen, "Towards the computational design of solid catalysts," *Nature chemistry*, vol. 1, no. 1, p. 37, 2009.

[24] B. Hammer and J. Nørskov, "Electronic factors determining the reactivity of metal surfaces," *Surface Science*, vol. 343, no. 3, pp. 211–220, 1995.

[25] E. A. Walker, D. Mitchell, G. A. Terejanu, and A. Heyden, "Identifying active sites of the water–gas shift reaction over titania supported platinum catalysts under uncertainty," *ACS Catalysis*, vol. 8, no. 5, pp. 3990–3998, 2018.

[26] M. Ernzerhof and G. E. Scuseria, "Assessment of the perdew–burke–ernzerhof exchange-correlation functional," *The Journal of chemical physics*, vol. 110, no. 11, pp. 5029–5036, 1999.

[27] E. Walker, S. C. Ammal, G. A. Terejanu, and A. Heyden, "Uncertainty quantification framework applied to the water–gas shift reaction over pt-based catalysts," *The Journal of Physical Chemistry C*, vol. 120, no. 19, pp. 10328–10339, 2016.

[28] Z. W. Ulissi, A. J. Medford, T. Bligaard, and J. K. Nørskov, "To address surface reaction network complexity using scaling relations machine learning and dft calculations," *Nature communications*, vol. 8, p. 14621, 2017.

[29] P. Biloen, "Transient kinetic methods," *Journal of Molecular Catalysis*, vol. 21, no. 1-3, pp. 17–24, 1983.

[30] G. S. Yablonsky, E. A. Redekop, D. Constales, J. T. Gleaves, and G. B. Marin, "Rate-reactivity model: A new theoretical basis for systematic kinetic characterization of heterogeneous catalysts," *International Journal of Chemical Kinetics*, vol. 48, no. 6, pp. 304–317, 2016.

[31] K. Morgan, N. Maguire, R. Fushimi, J. Gleaves, A. Goguet, M. Harold, E. Kondratenko, U. Menon, Y. Schuurman, and G. Yablonsky, "Forty years of temporal analysis of products," *Catalysis Science & Technology*, vol. 7, no. 12, pp. 2416–2439, 2017.

[32] J. T. Gleaves, J. Ebner, and T. Kuechler, "Temporal analysis of products (tap)—a unique catalyst evaluation system with submillisecond time resolution," *Catalysis Reviews Science and Engineering*, vol. 30, no. 1, pp. 49–116, 1988.

[33] J. T. Gleaves, G. S. Yablonskii, P. Phanawadee, and Y. Schuurman, "Tap-2: An interrogative kinetics approach," *Applied Catalysis A: General*, vol. 160, no. 1, pp. 55–88, 1997.

[34] S. Shekhtman, G. Yablonsky, S. Chen, and J. Gleaves, "Thin-zone tap-reactor–theory and application," *Chemical Engineering Science*, vol. 54, no. 20, pp. 4371–4378, 1999.

[35] G. Yablonsky, D. Constales, S. Shekhtman, and J. Gleaves, "The y-procedure: How to extract the chemical transformation rate from reaction–diffusion data with no assumption on the kinetic model," *Chemical Engineering Science*, vol. 62, no. 23, pp. 6754–6767, 2007.

[36] E. A. Redekop, G. S. Yablonsky, D. Constales, P. A. Ramachandran, C. Pherigo, and J. T. Gleaves, "The y-procedure methodology for the interpretation of transient kinetic data: Analysis of irreversible adsorption," *Chemical engineering science*, vol. 66, no. 24, pp. 6441–6452, 2011.

[37] B. Golman, "Transient kinetic analysis of multipath reactions: An educational module using the ipython software package," *Education for Chemical Engineers*, vol. 15, pp. 1–18, 2016.

[38] E. A. Redekop, G. S. Yablonsky, V. V. Galvita, D. Constales, R. Fushimi, J. T. Gleaves, and G. B. Marin, "Momentary equilibrium in transient kinetics and its application for estimating the concentration of catalytic sites," *Industrial & Engineering Chemistry Research*, vol. 52, no. 44, pp. 15417–15427, 2013.

[39] A. G. Baydin, B. A. Pearlmutter, A. A. Radul, and J. M. Siskind, "Automatic differentiation in machine learning: a survey," *arXiv preprint arXiv:1502.05767*, 2015.

[40] A. Dürrbaum, W. Klier, and H. Hahn, "Comparison of automatic and symbolic differentiation in mathematical modeling and computer simulation of rigid-body systems," *Multibody System Dynamics*, vol. 7, no. 4, pp. 331–355, 2002.

[41] J. Cheng, X. Jia, and Y. Wang, "Numerical differentiation and its applications," *Inverse problems in Science and Engineering*, vol. 15, no. 4, pp. 339–357, 2007.

[42] L. B. Rall, "Automatic differentiation: Techniques and applications," 1981.

[43] M. Sambridge, P. Rickwood, N. Rawlinson, and S. Sommacal, "Automatic differentiation in geophysical inverse problems," *Geophysical Journal International*, vol. 170, no. 1, pp. 1–8, 2007.

[44] C. Homescu, "Adjoints and automatic (algorithmic) differentiation in computational finance," 2011.

[45] M. S. Alnæs, J. Blechta, J. Hake, A. Johansson, B. Kehlet, A. Logg, C. Richardson, J. Ring, M. E. Rognes, and G. N. Wells, "The fenics project version 1.5," *Archive of Numerical Software*, vol. 3, no. 100, 2015.

[46] A. Logg and G. N. Wells, "Dolfin: Automated finite element computing," *ACM Transactions on Mathematical Software (TOMS)*, vol. 37, no. 2, p. 20, 2010.

[47] A. Logg, G. N. Wells, and J. Hake, *DOLFIN: a C++/Python Finite Element Library*, ch. 10. Springer, 2012.

[48] P. E. Farrell, D. A. Ham, S. W. Funke, and M. E. Rognes, "Automated derivation of the adjoint of high-level transient finite element programs," *SIAM Journal on Scientific Computing*, vol. 35, no. 4, pp. C369–C393, 2013.

[49] S. W. Funke and P. E. Farrell, "A framework for automated pde-constrained optimisation," *arXiv preprint arXiv:1302.3894*, 2013.

[50] A. Griewank and A. Walther, "Algorithm 799: revolve: an implementation of checkpointing for the reverse or adjoint mode of computational differentiation," *ACM Transactions on Mathematical Software (TOMS)*, vol. 26, no. 1, pp. 19–45, 2000.

[51] M. S. Alnæs, A. Logg, K. B. Ølgaard, M. E. Rognes, and G. N. Wells, "Unified form language: A domain-specific language for weak formulations of partial differential equations," *ACM Transactions on Mathematical Software (TOMS)*, vol. 40, no. 2, p. 9, 2014.

[52] S. Balay, S. Abhyankar, M. Adams, J. Brown, P. Brune, K. Buschelman, L. Dalcin, A. Dener, V. Eijkhout, W. Gropp, *et al.*, "Petsc users manual: Revision 3.10," tech. rep., Argonne National Lab.(ANL), Argonne, IL (United States), 2018.

[53] M. Sheraton and P. M. Sloot, "Parallel performance analysis of bacterial biofilm simulation models," in *International Conference on Computational Science*, pp. 496–505, Springer, 2018.

[54] S. Natarajan, R. K. Annabattula, *et al.*, "A fenics implementation of the phase field method for quasi-static brittle fracture," *Frontiers of Structural and Civil Engineering*, pp. 1–17.

[55] Q. Hong, J. Kraus, M. Lymbery, and F. Philo, "Conservative discretizations and parameter-robust preconditioners for biot and multiple-network flux-based poroelastic models," *arXiv preprint arXiv:1806.00353*, 2018.

[56] J.-C. Croix, N. Durrande, and M. Alvarez, "Bayesian inversion of a diffusion evolution equation with application to biology," *arXiv preprint arXiv:1806.05843*, 2018.

[57] M. Nauheimer, R. Relan, U. H. Thygesen, H. Madsen, B. Olesen, K. Kirkeby, and D. Compute, "A stochastic spatio-temporal model of the flow-front dynamics in a vacuum assisted resin transfer moulding process," in *18th IFAC Symposium on System Identification, SYSID*, vol. 2018, pp. 1–6, 2018.

[58] X. Li, D. J. Buttrey, D. A. Blom, and T. Vogt, "Improvement of the structural model for the m1 phase mo–v–nb–te–o propane (amm) oxidation catalyst," *Topics in Catalysis*, vol. 54, no. 10-12, p. 614, 2011.

[59] M. R. Kunz, T. Borders, E. Redekop, G. S. Yablonsky, D. Constales, L. Wang, and R. Fushimi, "Pulse response analysis using the y-procedure: A data science approach," *Chemical Engineering Science*, vol. 192, pp. 46–60, 2018.

[60] S. Rangarajan, A. Bhan, and P. Daoutidis, "Language-oriented rule-based reaction network generation and analysis: Description of ring," *Computers & Chemical Engineering*, vol. 45, pp. 114–123, 2012.

[61] C. F. Goldsmith and R. H. West, "Automatic generation of microkinetic mechanisms for heterogeneous catalysis," *The Journal of Physical Chemistry C*, vol. 121, no. 18, pp. 9970–9981, 2017.

[62] C. W. Gao, J. W. Allen, W. H. Green, and R. H. West, "Reaction mechanism generator: Automatic construction of chemical kinetic mechanisms," *Computer Physics Communications*, vol. 203, pp. 212–225, 2016.

[63] N. M. O'Boyle, C. Morley, and G. R. Hutchison, "Pybel: a python wrapper for the openbabel cheminformatics toolkit," *Chemistry Central Journal*, vol. 2, no. 1, p. 5, 2008.

[64] A. Hagberg, D. Schult, P. Swart, D. Conway, L. Séguin-Charbonneau, C. Ellison, B. Edwards, and J. Torrents, "Networkx. high productivity software for complex networks," *Webová strá nka https://networkx. lanl. gov/wiki*, 2013.

[65] R. Shields, "Cultural topology: The seven bridges of königsburg, 1736," *Theory, Culture & Society*, vol. 29, no. 4-5, pp. 43–57, 2012.

[66] J. J. Sylvester, "On an application of the new atomic theory to the graphical representation of the invariants and covariants of binary quantics, with three appendices," *American Journal of Mathematics*, vol. 1, no. 1, pp. 64–104, 1878.

[67] J. E. Sutton and D. G. Vlachos, "Building large microkinetic models with first-principles accuracy at reduced computational cost," *Chemical Engineering Science*, vol. 121, pp. 190–199, 2015.

[68] A. Meurer, C. P. Smith, M. Paprocki, O. Čertík, S. B. Kirpichev, M. Rocklin, A. Kumar, S. Ivanov, J. K. Moore, S. Singh, T. Rathnayake, S. Vig, B. E. Granger, R. P. Muller, F. Bonazzi, H. Gupta, S. Vats, F. Johansson, F. Pedregosa, M. J. Curry, A. R. Terrel, v. Roučka, A. Saboo, I. Fernando, S. Kulal, R. Cimrman, and A. Scopatz, "Sympy: symbolic computing in python," *PeerJ Computer Science*, vol. 3, p. e103, Jan. 2017.

[69] D. Constales, G. Yablonsky, G. Marin, and J. Gleaves, "Multi-zone tap-reactors theory and application: I. the global transfer matrix equation," *Chemical Engineering Science*, vol. 56, no. 1, pp. 133–149, 2001.

[70] J. T. Gleaves, G. Yablonsky, X. Zheng, R. Fushimi, and P. L. Mills, "Temporal analysis of products (tap)—recent advances in technology for kinetic analysis of multi-component catalysts," *Journal of Molecular Catalysis A: Chemical*, vol. 315, no. 2, pp. 108–134, 2010.

[71] A. Logg, K.-A. Mardal, and G. Wells, *Automated solution of differential equations by the finite element method: The FEniCS book*, vol. 84. Springer Science & Business Media, 2012.

[72] E. A. Redekop, G. S. Yablonsky, D. Constales, P. A. Ramachandran, J. T. Gleaves, and G. B. Marin, "Elucidating complex catalytic mechanisms based on transient pulse-response kinetic data," *Chemical Engineering Science*, vol. 110, pp. 20–30, 2014.

[73] C. T. Campbell, "Finding the rate-determining step in a mechanism: comparing dedonder relations with the "degree of rate control"," 2001.

[74] C. T. Campbell, "The degree of rate control: a powerful tool for catalysis research," 2017.

[75] C. A. Wolcott, A. J. Medford, F. Studt, and C. T. Campbell, "Degree of rate control approach to computational catalyst screening," *Journal of catalysis*, vol. 330, pp. 197–207, 2015.

[76] S. C. van der Linde, T. Nijhuis, F. Dekker, F. Kapteijn, and J. A. Moulijn, "Mathematical treatment of transient kinetic data: combination of parameter estimation with solving the related partial differential equations," *Applied Catalysis A: General*, vol. 151, no. 1, pp. 27–57, 1997.

[77] Y. Schuurman, "Assessment of kinetic modeling procedures of tap experiments," *Catalysis Today*, vol. 121, no. 3-4, pp. 187–196, 2007.

[78] V. Balcaen, I. Sack, M. Olea, and G. Marin, "Transient kinetic modeling of the oxidative dehydrogenation of propane over a vanadia-based catalyst in the absence of o2," *Applied Catalysis A: General*, vol. 371, no. 1-2, pp. 31–42, 2009.

[79] E. V. Kondratenko and J. Pérez-Ramírez, "Micro-kinetic analysis of direct n2o decomposition over steam-activated fe-silicalite from transient experiments in the tap reactor," *Catalysis Today*, vol. 121, no. 3-4, pp. 197–203, 2007.

[80] A. Heyden, B. Peters, A. T. Bell, and F. J. Keil, "Comprehensive dft study of nitrous oxide decomposition over fe-zsm-5," *The Journal of Physical Chemistry B*, vol. 109, no. 5, pp. 1857–1873, 2005.

[81] D. Wolf and R. Moros, "Estimating rate constants of heterogeneous catalytic reactions without supposition of rate determining surface steps—an application of a genetic algorithm," *Chemical Engineering Science*, vol. 52, no. 7, pp. 1189–1199, 1997.

[82] M. Soick, D. Wolf, and M. Baerns, "Determination of kinetic parameters for complex heterogeneous catalytic reactions by numerical evaluation of tap experiments," *Chemical engineering science*, vol. 55, no. 15, pp. 2875–2882, 2000.

[83] W. H. Press, S. A. Teukolsky, W. T. Vetterling, and B. P. Flannery, *Numerical recipes in Fortran 90*, vol. 2. Cambridge university press Cambridge, 1996.

[84] C. Reece, E. A. Redekop, S. Karakalos, C. M. Friend, and R. J. Madix, "Crossing the great divide between single-crystal reactivity and actual catalyst selectivity with pressure transients," *Nature Catalysis*, vol. 1, no. 11, p. 852, 2018.

[85] I. Block, "Siam workshop on automatic differentiation of algorithms: Theory, implementation and application," tech. rep., SOCIETY FOR INDUSTRIAL AND APPLIED MATHEMATICS PHILADELPHIA PA, 1991.

[86] A. Savara, "Simulation and fitting of complex reaction network tpr: The key is the objective function," *Surface Science*, vol. 653, pp. 169–180, 2016.

[87] S. Surnev, M. Ramsey, and F. Netzer, "Vanadium oxide surface studies," *Progress in surface science*, vol. 73, no. 4-8, pp. 117–165, 2003.

[88] M.-J. Cheng and W. A. Goddard, "The mechanism of alkane selective oxidation by the m1 phase of mo–v–nb–te mixed metal oxides: Suggestions for improved catalysts," *Topics in Catalysis*, vol. 59, no. 17-18, pp. 1506–1517, 2016.

[89] R. K. Grasselli, "Selectivity issues in (amm) oxidation catalysis," *Catalysis Today*, vol. 99, no. 1-2, pp. 23–31, 2005.

[90] M. Ek, Q. M. Ramasse, L. Arnarson, P. G. Moses, and S. Helveg, "Visualizing atomic-scale redox dynamics in vanadium oxide-based catalysts," *Nature communications*, vol. 8, no. 1, p. 305, 2017.

[91] R. J. Berger, F. Kapteijn, J. A. Moulijn, G. B. Marin, J. De Wilde, M. Olea, D. Chen, A. Holmen, L. Lietti, E. Tronconi, *et al.*, "Dynamic methods for catalytic kinetics," *Applied Catalysis A: General*, vol. 342, no. 1-2, pp. 3–28, 2008.

[92] R. J. Berger, E. H. Stitt, G. B. Marin, F. Kapteijn, and J. A. Moulijn, "Eurokin. chemical reaction kinetics in practice," *Cattech*, vol. 5, no. 1, pp. 36–60, 2001.

[93] W. E. Schiesser, *The numerical method of lines: integration of partial differential equations*. Elsevier, 2012.

[94] A. C. Hindmarsh, "Odepack, a systematized collection of ode solvers, rs stepleman et al," *IMACS Trans, on Scientific Computation*, vol. 1, 1983.

[95] M. C. Seiler and F. A. Seiler, "Numerical recipes in c: the art of scientific computing," *Risk Analysis*, vol. 9, no. 3, pp. 415–416, 1989.

[96] W. Stewart and M. Caracotsios, "Athena visual studio," 2010.

[97] M. Simo, C. J. Brown, and V. Hlavacek, "Simulation of pressure swing adsorption in fuel ethanol production process," *Computers & Chemical Engineering*, vol. 32, no. 7, pp. 1635–1649, 2008.

[98] Y. Liu, J. Delgado, and J. A. Ritter, "Comparison of finite difference techniques for simulating pressure swing adsorption," *Adsorption*, vol. 4, no. 3-4, pp. 337–344, 1998.

[99] Y. Liu and J. A. Ritter, "Evaluation of model approximations in simulating pressure swing adsorption- solvent vapor recovery," *Industrial & engineering chemistry research*, vol. 36, no. 5, pp. 1767–1778, 1997.

[100] J. A. Ritter and R. T. Yang, "Pressure swing adsorption: experimental and theoretical study on air purification and vapor recovery," *Industrial & Engineering Chemistry Research*, vol. 30, no. 5, pp. 1023–1032, 1991.

[101] M. Rudolph, D. P. Reddy, and S. W. Feldberg, "A simulator for cyclic voltammetric responses," *Analytical chemistry*, vol. 66, no. 10, pp. 589A–600A, 1994.

[102] D. K. Gosser, *Cyclic voltammetry: simulation and analysis of reaction mechanisms*, vol. 43. VCH New York, 1993.

[103] A. J. Medford, C. Shi, M. J. Hoffmann, A. C. Lausche, S. R. Fitzgibbon, T. Bligaard, and J. K. Nørskov, "Catmap: a software package for descriptor-based microkinetic mapping of catalytic trends," *Catalysis Letters*, vol. 145, no. 3, pp. 794–807, 2015.

[104] S. Lwin, W. Diao, C. Baroi, A. M. Gaffney, and R. R. Fushimi, "Characterization of movtenbox catalysts during oxidation reactions using in situ/operando techniques: A review," *Catalysts*, vol. 7, no. 4, p. 109, 2017.